UPPSALA
UNIVERSITET

Digital Comprehensive Summaries of Uppsala Dissertations from the Faculty of Science and Technology 1399

A tale of two antibiotics

Fusidic acid and Viomycin

MIKAEL HOLM

ACTA
UNIVERSITATIS
UPSALIENSIS
UPPSALA
2016

ISSN 1651-6214
ISBN 978-91-554-9644-9
urn:nbn:se:uu:diva-300479

Dissertation presented at Uppsala University to be publicly examined in B41 BMC, Husargatan 3, Uppsala, Friday, 23 September 2016 at 13:15 for the degree of Doctor of Philosophy. The examination will be conducted in English. Faculty examiner: Associate Professor Scott Blanchard (Cornell University, Department of Physiology and Biophysics).

Abstract
Holm, M. 2016. A tale of two antibiotics. Fusidic acid and Viomycin. *Digital Comprehensive Summaries of Uppsala Dissertations from the Faculty of Science and Technology* 1399. 64 pp. Uppsala: Acta Universitatis Upsaliensis. ISBN 978-91-554-9644-9.

Antibiotics that target the bacterial ribosome make up about half of all clinically used antibiotics. We have studied two ribosome targeting drugs: Fusidic acid and Viomycin. Fusidic acid inhibits bacterial protein synthesis by binding to elongation factor G (EF-G) on the ribosome, thereby inhibiting translocation of the bacterial ribosome. Viomycin binds directly to the ribosome and inhibits both the fidelity of mRNA decoding and translocation. We found that the mechanisms of inhibition of these two antibiotics were unexpectedly complex. Fusidic acid can bind to EF-G on the ribosome during three separate stages of translocation. Binding of the drug to the first and most sensitive state does not lead to stalling of the ribosome. Rather the ribosome continues unhindered to a downstream state where it stalls for around 8 seconds. Dissociation of fusidic acid from this state allows the ribosome to continue translocating but it soon reaches yet another fusidic acid sensitive state where it can be stalled again, this time for 6 seconds. Viomycin inhibits translocation by binding to the pre-translocation ribosome in competition with EF-G. If viomycin binds before EF-G it stalls the ribosome for 44 seconds, much longer than a normal elongation cycle. Both viomycin and fusidic acid probably cause long queues of ribosomes to build up on the mRNA when they bind. Viomycin inhibits translational fidelity by binding to the ribosome during initial selection. We found that the concentration of viomycin required to bind to the ribosome with a given probability during decoding is proportional to the accuracy of the codon·anticodon pair being decoded. This demonstrated that long standing models about ribosomal accuracy cannot be correct. Finally, we demonstrated that a common viomycin resistance mutation increases the drug binding rate and decreases its dissociation rate. Our results demonstrate that ribosome targeting drugs have unexpectedly complex mechanisms of action. Both fusidic acid and viomycin preferentially bind to conformations of the ribosome other than those that they stabilize. This suggests that determining the structures of stable drug-bound states may not give sufficient information for drug design.

Keywords: Protein Synthesis, Antibiotics, Fusidic acid, Viomycin, Translocation, Accuracy

Mikael Holm, Department of Cell and Molecular Biology, Structure and Molecular Biology, 596, Uppsala University, SE-751 24 Uppsala, Sweden.

ISSN 1651-6214
ISBN 978-91-554-9644-9
urn:nbn:se:uu:diva-300479 (http://urn.kb.se/resolve?urn=urn:nbn:se:uu:diva-300479)

“To those of you who received high honors, awards and distinctions, I say well done. And as I like to tell the C students: you too, can be president.”

George W. Bush

List of Papers

This thesis is based on the following papers, which are referred to in the text by their Roman numerals.

I Borg, A., **Holm**, **M**., Shiroyama, I., Hauryliuk, V., Pavlov, M., Sanyal, S., Ehrenberg, M. (2015) Fusidic acid targets elongation factor G in several stages of translocation on the bacterial ribosome. *The journal of Biological Chemistry*, 290(6):3440–3454

II **Holm**, **M**., Borg, A., Ehrenberg, M., Sanyal, S. (2016) Molecular mechanism of viomycin inhibition of peptide elongation in bacteria. *Proc Natl Acad Sci U S A*, 113(4):978-983

III **Holm**, **M**., Sanyal, S. Insights into the fidelity mechanism of mRNA decoding from characterization of viomycin induced miscoding in translation. (*Submitted Manuscript*)

IV **Holm**, **M**., Ge, X., Sanyal, S. Biochemical characterization of ΔTlyA mediated viomycin resistance. (*Manuscript*)

Reprints were made with permission from the respective publishers.

Papers not included in this thesis

Koripella, R. K., **Holm**, **M**., Dourado, D., Mandava, C. S., Flores, S., Sanyal, S. (2015) A conserved histidine in switch-II of EF-G moderates release of inorganic phosphate. *Sci Rep*, 5:12970

Korkmaz, G., **Holm**, **M**. Wiens, T., Sanyal, S. (2014) Comprehensive analysis of stop codon usage in bacteria and its correlation with release factor abundance. *The journal of Biological Chemistry*, 289(44):30334-30342

Contents

Abbreviations

30S	The small subunit of the bacterial ribosome
50S	The large subunit of the bacterial ribosome
70S	The intact bacterial ribosome
A	Adenine
AA	Amino Acid
ASL	Anticodon Stem Loop
C	Cytidine
EF	Elongation Factor
G	Guanine
GTP	Guanine triphosphate
IF	Initiation Factor
mRNA	Messenger RNA
ORF	Open Reading Frame
PTC	Peptidyl Transfer Center
RF	Release Factor
RRF	Ribosome Recycling Factor
rRNA	Ribosomal RNA
tRNA	Transfer RNA
U	Uracil

Introduction

Antibiotics are a fundamental part of modern civilization and without them many medical treatments that we take for granted would not be possible. For about a century now we have been using these highly effective drugs to stave of infectious disease caused primarily by pathogenic bacteria. The bacteria that are the target of these drugs are fighting back and an increasing number of infections are resistant to even our best antibiotics. This thesis is about two antibiotics, viomycin and fusidic acid, both of which target the bacterial ribosome. Ribosomes produce the proteins that make up nearly half of the mass of a bacterial cell. The proteins made by the ribosome carry out almost all vital functions in the cell from chemical catalysis to information processing, sensing of signals and even copying of the cell's genes during reproduction. The instructions for how to make all of these proteins are called genes and are stored in long molecules of DNA. The collection of all of the genes in an organism is called its genome. The ribosome does not read the genes in DNA directly, rather they are first copied, *transcribed*, into messenger RNA (mRNA) molecules by an enzyme called RNA polymerase. The information stored in the sequence of the mRNA molecule is then read and *translated* into protein by the ribosome. This idea that information flows from DNA to RNA to protein is called the central dogma of molecular biology. It takes place in all living organisms from humans to the lowliest bacterium.

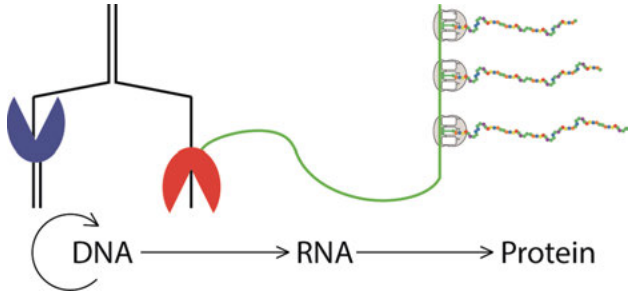

Figure 1. The central dogma of molecular biology. DNA is transcribed into RNA which is translated into protein. The DNA is copied during cell replication.

By far the most complex part of the central dogma is the translation of the information in mRNA molecules into protein molecules. The language of nucleic acids with only the four letters, Adenine (A), Uracil (U), Cytidine (C) and Guanine (G) has to be translated into the language of proteins made up of

the 20 naturally occurring amino acids. To accomplish this the ribosome reads the mRNA three nucleotides (letters) at a time, such a triplet is called a codon. The ribosome moves along the mRNA one codon at a time and for each codon it selects an amino acid carrying RNA adaptor molecule with a corresponding anticodon, called a transfer RNA (tRNA). Guided by the sequence of codons in the mRNA the ribosome strings together the amino acids from successive tRNAs into a long chain, a protein. The tRNAs thus form the bridge between the chemically distinct languages of nucleic acids and proteins. The 20 possible amino acids are each specified by at least one codon and many by several different codons in what is called the genetic code. The ribosome is under enormous evolutionary pressure to carry out this process both with great speed and with great accuracy. Part of this thesis will deal with how the ribosome achieves such high accuracy during translation.

This process of protein synthesis by the ribosome is highly conserved between different organisms, even bacterial and human ribosomes are quite similar. In spite of this many of the antibiotics used by us to combat infectious bacteria are inhibitors of protein synthesis and bind to the ribosome. Despite the crucial importance of many antibiotics surprisingly few details are known about their function. The work in this thesis was prompted in part by a desire to quantitatively characterize some of these drugs as what they really are, inhibitors of the most complex enzymatic reaction in the cell. I will begin the thesis by outlining the molecular biology of protein synthesis in bacteria, with particular focus on the accuracy of translation and the process of translocation – two of the processes inhibited by the antibiotics, viomycin and fusidic acid. Then will follow a description of the methods used to produce the results in our experimental studies and finally a discussion of the results themselves.

Molecular biology of bacterial translation

The bacterial ribosome

The bacterial ribosome is a giant enzyme that carries out all of the chemical reactions involved in mRNA translation. The ribosome does not carry out translation alone, but requires its substrates the tRNAs, multiple helper proteins called translation factors and the aminoacyl-tRNA synthetases that charge the tRNAs with the appropriate amino acids. With a mass of 2.5 MDa the ribosome is one of the largest macromolecular assemblies in the cell. Together with all of the translation factors, tRNAs and other associated proteins a large portion of all the energy and mass produced by the cell is used by the protein synthesis machinery [1, 2]. The intact bacterial ribosome is called the 70S ribosome (the S here is the Svedberg unit of sedimentation). Each 70S ribosome is made up of two subunits, the large 50S subunit and the small 30S subunit. The 30S subunit consists of one RNA molecule of 1540 nucleotides,

the 16S ribosomal RNA (rRNA), and 21 proteins. The 50S subunit consists of two RNA molecules, the 120 nucleotide 5S rRNA and the 2900 nucleotide 23S rRNA, as well as some 31 proteins. These numbers vary between different bacterial species, but this thesis is primarily concerned with *E. coli* ribosomes for which they are accurate.

During protein synthesis there is a division of labor between the two ribosomal subunits. The mRNA interacts only with the 30S subunit so it is on this subunit that the genetic code is actually read. The 50S subunit contains the peptidyl transferase center (PTC), where the chemical catalysis of joining amino acids together takes place. Each subunit has three partial tRNA binding sites, that combine into full binding sites when the subunits are joined in the 70S ribosome. The Acceptor (A), Peptidyl (P) and Exit (E) sites [3]. During translation tRNAs move through these three binding sites as the ribosome moves along the mRNA and amino acids are added to the nascent peptide chain.

The structures of the two ribosomal subunits were determined at atomic resolution in the year 2000 [4-6]. Since then a large number of additional structures of the intact ribosome in complex with various ligands, mRNA, tRNA and translation factors have been determined. As this thesis is about functional rather than structural studies of translation we will make do with a much lower resolution "structure" of the ribosome most of the time.

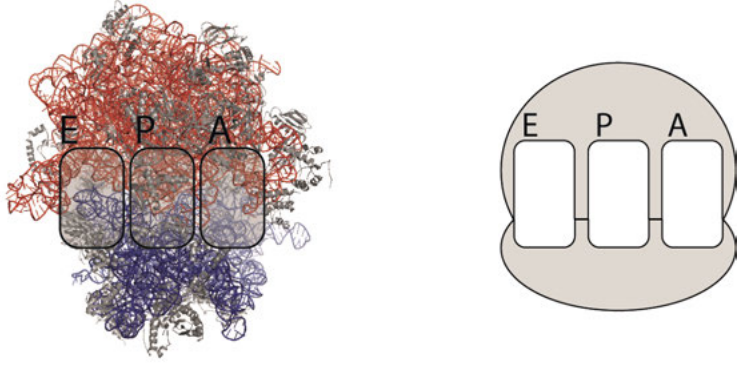

Figure 2. The bacterial ribosome. On the left is an accurate view of the ribosome taken from an atomic resolution cryo electron microscopy (cryo-EM) structure (PDB entry 5AFI [7]). The 23S rRNA is shown in red, the 16S rRNA in blue and the ribosomal proteins in grey. On the right is a low resolution drawing of the ribosome that we will use throughout this thesis. The three tRNA binding sites are indicated in both images.

Protein synthesis

To understand how antibiotics interfere with bacterial translation we must first have an idea of how protein synthesis itself is carried out. Bacterial protein synthesis can be split into four phases: initiation, elongation, termination and recycling. In this section, I will give a brief overview of the molecular details of these four phases as well as a small glimpse into the role of the ribosome in the folding of the proteins that it produces. Bacterial translation occurs at a blinding pace. By the time you have finished reading this paragraph a bacterial ribosome could have synthesized an entire protein (well a small one), carrying out a hundred cycles of elongation and one of each of the other steps described below [2, 8].

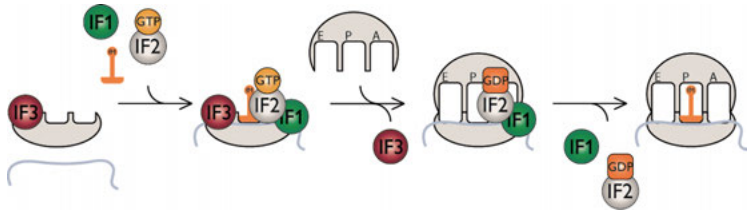

Figure 3. Initiation of protein synthesis in bacteria.

Initiation

Initiation is the first step in synthesis of a new protein. It begins when the 30S subunit bound to initiation factor 3 (IF3) binds to the beginning of an open reading frame (ORF) on an mRNA molecule. Then follows binding of Initiation factor 1 and Initiation factor 2 in complex with GTP (IF1 and IF2(GTP)). Finally, the special initiator $tRNA^{fMet}$, carrying an N-formylated version of the amino acid methionine, binds to the 30S subunit to complete the formation of the 30S pre-initiation complex (PIC). The presence of a tRNA in the P-site destabilizes IF3 in the PIC causing the factor to spontaneously dissociate [9]. IF3 in turn destabilizes tRNAs in the P site, thereby increasing the accuracy of initiation by increasing the dissociation rate of both initiatior and elongator tRNAs from the PIC [10]. IF2 specifically recognizes the initiator tRNA and the formyl group on the methionine residue which shifts the conformation of IF2(GTP) to its active GTP conformation [11]. The 50S subunit rapidly docks to the now IF3-free 30S PIC with active IF2(GTP) [11]. This triggers GTP hydrolysis by IF2 followed by dissociation of IF1 and IF2(GDP), readying the ribosome for elongation [12]. This description sounds pretty complete, but initiation is perhaps the least understood area in translation. The actual sequence of events, and in particular the role of IF3, is contested. But perhaps more importantly it is unknown how the ribosome actually finds a start codon *in vivo* and what determines the initiation rate of a given ORF [13, 14].

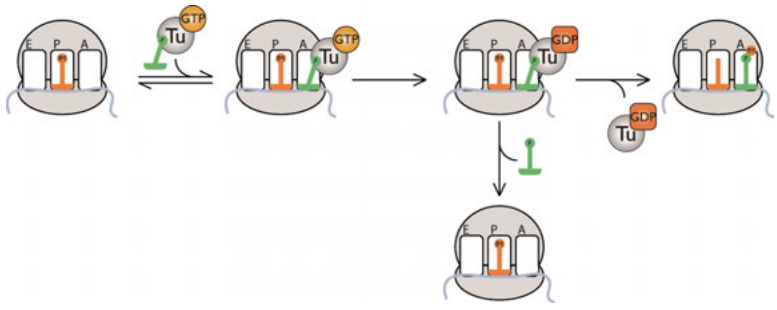

Figure 4. The first half of the elongation cycle. Decoding of the mRNA codon in the A site.

Elongation I: Decoding

After initiation the ribosome enters the first half of the elongation cycle where it reads the mRNA codon presented in the ribosomal A site and selects the appropriate aminoacyl-tRNA (AA-tRNA). AA-tRNAs are delivered to the ribosome in ternary complex with the GTPase Elongation factor Tu (EF-Tu) and GTP. Ternary complexes bind to the ribosome so that the anticodon stem loop (ASL) of the tRNA can reach the codon in the 30S A site while the body of the tRNA is still bound to EF-Tu (called the A/T state). This prevents entry of the aminoacyl arm of the tRNA into the 50S A site and the PTC [15]. If the nucleotide sequence of the codon is complementary to the anticodon the tRNA is accepted by the ribosome by triggering of GTP hydrolysis by EF-Tu. EF-Tu then dissociates from the ribosome leaving the AA-tRNA in the A site. This is followed by rapid accommodation of the AA-tRNA into the PTC. In the PTC the nascent peptide chain is transferred from the P-site tRNA to the amino acid on the newly arrived A-site tRNA, extending the growing protein by one amino acid. If the codon and the anticodon do not match the tRNA is rejected. Rejection can happen both before GTP hydrolysis by dissociation of the ternary complex or, in a process called proofreading, after GTP hydrolysis but before accommodation into the PTC by dissociation of the tRNA either on its own or together with EF-Tu(GDP). It is crucial that the decoding process is both fast, as the ribosome spends the majority of its time elongating protein chains, and accurate, so that the sequence of codons in the mRNA is faithfully translated into the corresponding protein sequence. Exactly how fast, and how accurate is a hotly contested topic in translation research, as is how this speed and accuracy is achieved [16]. It is believed that how quickly a codon is decoded is proportional to the free concentration of ternary complexes containing tRNAs matched for that codon. However, no such direct correlation has been observed *in vivo* by ribosome profiling experiments [17, 18]. Decoding will be given greater attention later on in this thesis, in particular the mechanism by which the ribosome achieves its remarkable accuracy.

Figure 5. The second half of the elongation cycle. Translocation of the two tRNAs and the mRNA through the ribosome by one codon.

Elongation II: Translocation

After decoding the ribosome enters into the second half of the elongation cycle where the new peptidyl tRNA in the A site must move to the P site and the deacylated tRNA in the P site must move to the E site. After peptidyl transfer the ribosome begins to fluctuate between what is called the non-rotated and rotated [19, 20] states (or locked and unlocked, non-ratcheted and ratcheted, macrostate 1 and macrostate 2 and so on…). When going from the non-rotated to the rotated state the ribosomal subunits rotate clockwise with respect to each other by about 10º [21, 22] and the tRNAs enter the A/P and P/E hybrid states [20]. In the hybrid states the acceptor stem of the A-site tRNA has moved into the 50S P site and the acceptor stem of the P-site tRNA has moved to the 50S E site while the anticodon stem loops (ASLs) of both tRNA remain in their respective binding sites on the 30S subunit. While the ribosome is fluctuating between these two conformations EF-G binds. Whether EF-G binds only to the rotated ribosome or can induce rotation of the non-rotated ribosome is unclear but its binding stabilizes the rotated state [23-25]. While bound to the ribosome EF-G catalyzes the translocation process, which still occurs in the absence of EF-G although very slowly [26, 27]. How EF-G performs this catalysis is largely unknown. In particular, the role of GTP hydrolysis by EF-G is unclear. Some authors suggest that GTP hydrolysis is pre-translocational and that EF-G acts as a motor protein that uses the free energy from GTP hydrolysis to push the mRNA and tRNAs through the ribosome [28-30]. Others suggest that GTP is hydrolyzed after the mRNA and tRNAs have moved to dislodge EF-G from the ribosome [31]. Experiments showing that non-hydrolysable GTP analogs [32, 33] or even GDP with P_i analogs [34] affect the rate of mRNA movement by less than one order of magnitude seem to argue against the motor protein model. No consensus exists and recently hybrid models have been proposed [35, 36]. During translocation the ribosome undergoes a large number of conformational rearrangements [37, 38]. The two subunits rotate by about 10º in relation to each other [22, 32], a domain of the 30S subunit called the 30S head rotates (swivels) in relation to the rest of the 30S by about 20º [39, 40], a part of the 50S subunit called the L1 stalk moves in and out of the E site [41] and of course the tRNA and mRNA molecules move by precisely one codon through the ribosome. The exact order and significance of these conformational changes is unknown. Ribosomes that are unable to rotate their subunits are unable to translocate [42] while ribosomes

lacking the L1 stalk are viable *in vivo* but translocate at lower rates [43]. How the ribosome manages to move by exactly one codon and what determines the rate of translocation at a given mRNA position is also unknown [17, 44]. When translocation is completed the ribosome is left with an empty A site presenting a new codon for decoding.

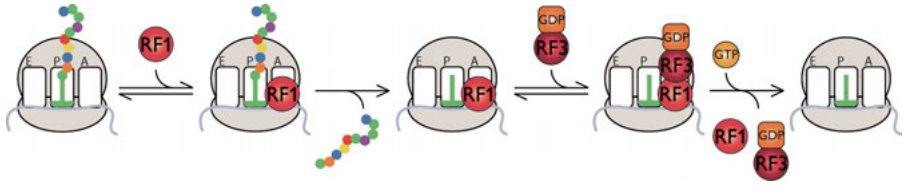

Figure 6. Termination of protein synthesis in bacteria.

Termination

After going through multiple elongation cycles the ribosome will reach the end of the ORF by arriving at the stop codon. Stop codons lack matching tRNA molecules and are instead read by the two class 1 protein release factors RF1 and RF2. There are three stop codons in total: UAA, UAG and UGA. UAA can be read by both release factors while UAG is read only by RF1 and UGA is read only by RF2 [45]. These three codons are used at widely varying frequencies by different bacteria [46, 47]. This is partially explained by genomic GC content but the codon UAG is almost always used by only 20% of all protein coding genes regardless of genome size and GC content. The class 1 release factors bind to the ribosomal A site, read the stop codon and cleave the ester bond between the P-site tRNA and the nascent protein chain. Releasing the nascent chain into the cytoplasm (or the membrane etc) to begin its life as a newly formed protein. The complex formed between the post-cleavage ribosome and either of the class 1 release factors is very stable and the action of the class 2 release factor RF3 is required to dislodge the class 1 release factors and prepare the ribosome for recycling [48]. RF3 is a GTPase but the driving force for class I release factor dissociation comes from exchange of RF3-bound GDP to GTP rather than from GTP hydrolysis [49]. GTP hydrolysis occurs before dissociation of RF3 from the ribosome.

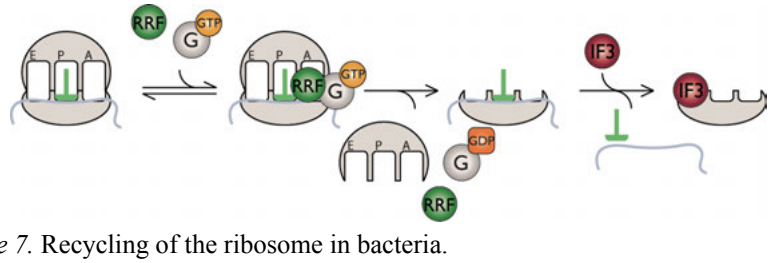

Figure 7. Recycling of the ribosome in bacteria.

Recycling

After termination the ribosome is left with a deacylated tRNA in the P site and an empty A site. To be ready for another round of protein synthesis the ribosome now needs to be recycled, by splitting of the 70S ribosome into the 30S and 50S subunits. Recycling is carried out by two proteins, Ribosome recycling factor (RRF) and EF-G (of translocation fame) [50]. The complete mechanism of ribosomal recycling was recently solved by the Ehrenberg lab [51]. Both RRF and EF-G can bind to the post termination ribosome independently of each other, but productive splitting of the ribosome requires that RRF is present prior to EF-G binding. Should EF-G bind first it leads only to unproductive GTP hydrolysis and dissociation of EF-G from the ribosome. This leads to a situation where maximizing the rate of recycling (and minimizing its energetic cost) requires very high free concentration of both RRF and EF-G *and* much higher free concentration of RRF than of EF-G. After the 50S subunit has been split from the 30S subunit the tRNA has to dissociate from the 30S P site and the 30S subunit has to dissociate from the mRNA. Why the ribosome has to be split into subunits at the end of translating an ORF is unclear. RRF is an essential protein in *E. coli* [52], but cells with unsplittable ribosomes are apparently viable [53, 54]. It has also been reported that intact 70S ribosomes are capable of initiation [55].

Folding

While this function of the ribosome has been controversial (though what novel finding is not) it now seems clear that the 50S subunit of the ribosome can act as a chaperone, aiding in the folding of proteins [56, 57]. This function would likely be carried out after splitting of the subunits, for instance on the newly released nascent protein chain, or on nascent chains being released from trailing ribosomes on the same mRNA. The exact molecular mechanism of this protein folding activity of the ribosome is unclear, but involvement of specific nucleotides in 23S rRNA have been implicated by mutational and crosslinking studies [58]. In addition to this direct folding activity the ribosome has been suggested to indirectly affect co-translational folding of the protein chain during elongation, specifically through modulation of the elongation rate [59-62].

The ribosome as a drug target

The bacterial ribosome is the target of around half of all clinically used antibiotics. As a target for antibiotic drugs the ribosome is both good, because its activity is crucial for cell proliferation, and bad because its structure is highly conserved between all kingdoms of life and therefore bacterial ribosomes and human ribosomes are rather similar. This is reflected by the often unparalleled bactericidal and bacteriostatic activities of many ribosome targeting drugs, but

also in their often equally unparalleled side effects. Even though there are dozens of antibiotic families that target the ribosome the number of drug binding sites is surprisingly small and many different drugs bind at the same site [63, 64]. In general, the sites of drug binding coincide with the major functional sites in the ribosome. For instance, aminoglycosides and tuberactinomycins bind at the decoding center, pleuromutilins and oxazolidinones bind in the PTC and macrolides and streptogramins bind in the exit tunnel. Two antibiotics, kirromycin and fusidic acid, bind to translation factors on the ribosome rather than to the ribosome itself, EF-Tu and EF-G respectively. Most ribosome-targeting drugs inhibit elongation, only a few inhibit initiation or recycling and none appear to inhibit termination [65]. The reason for this is probably that ribosomes spend most of their time going through the elongation cycle [2]. Thus elongating ribosomes make up the most abundant target for ribosome binding antibiotics.

Viomycin

Viomycin is the subject of papers II, III and IV. It is a member of the tuberactinomycin class of antibiotics and was discovered more than six decades ago in 1951 [66, 67]. It is a cyclic peptide (Figure 8) naturally produced by the bacterium *Streptomyces puniceus*. Unusually for a peptide it is not synthesized by the ribosome but rather by a set of protein enzymes [68]. Viomycin is almost exclusively used against multi-drug resistant tuberculosis (nowadays another drug from the same family, capreomycin, is commonly used instead). Its almost exclusive use against this illness is both because of the high sensitivity of *M. tuberculosis* to the drug and viomycin's severe side effects. Like the more well-known aminoglycosides viomycin causes missense errors in translation [69] and inhibits translocation [70]. Unlike the aminoglycosides viomycin is bacteriostatic rather than bactericidal. Viomycin binds near the ribosomal A site in a pocket formed between helix 44 (h44) of the small subunit and helix 69 (H69) of the large subunit when a tRNA is bound to the A site [71]. Binding of viomycin has been shown to stabilize the rotated state of the ribosome and the hybrid state of the A-site and P-site tRNAs [72]. However, there are conflicting reports on exactly which tRNA states are stabilized by viomycin and crystal structures of the ribosome in both the non-rotated [71] and the rotated [73, 74] states with viomycin bound exist. While viomycin inhibits translocation it does not inhibit binding of EF-G and a cryo-EM reconstruction of an EF-G bound viomycin-stalled pre-translocation ribosome exists [74]. In paper II we constructed a full kinetic model for the effect of viomycin on translocation, in paper III we investigated its effects on the accuracy of translation and finally in paper IV we studied the biochemical effect of a common viomycin resistance mutation.

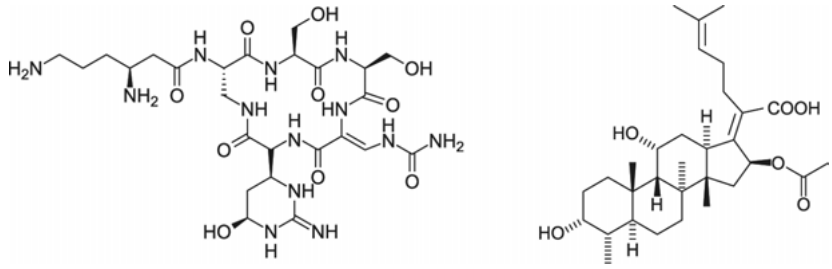

Figure 8. The chemical structures of viomycin on the left and fusidic acid on the right.

Fusidic acid

Fusidic acid is the subject of paper I, it is a steroid antibiotic that was discovered in 1962 [75] and is naturally produced by the fungus *Fusidium coccineum*. Fusidic acid is a bacteriostatic antibiotic that is used primarily to treat skin and eye infections of methicillin resistant *Staphylococcus aureus* (the infamous MRSA). Unlike viomycin, fusidic acid has no serious side effects and is still in clinical use today. It inhibits both ribosome recycling [50] and the release of EF-G after translocation [76] by binding to EF-G on the ribosome after GTP hydrolysis. Fusidic acid has almost no affinity for EF-G in solution but forms a very tight complex with the factor on the ribosome. It binds in a pocket close to the nucleotide binding site between domains I, II and III of EF-G after GTP hydrolysis by the factor [77]. Crystal and cryo-EM structures of the fusidic acid bound-ribosome EF-G complex have shown that possibly two distinct structures are stabilized by fusidic acid. One post-translocational with the tRNAs in the P/P and E/E states [77] and one intermediate translocation state with the tRNAs in so called chimeric hybrid states ap/P and pe/E [78]. In paper I we constructed a complete kinetic model for fusidic acid inhibition of translocation and show that it does stall the ribosome in two different states consistent with the structural data.

Translational accuracy

During decoding, the ribosome has to react only with correct substrates in a sea of incorrect ones. *In vivo* it does this both rapidly, performing up to 20 elongation cycles per second [2, 8] and accurately, with an average specific error frequency in the range of 10^{-4} to 10^{-3} [79], though with large fluctuations from codon to codon [80, 81].

In general, the accuracy of an enzymatic reaction is defined as the ratio of the steady state flows of correct and incorrect substrates into product, J^c and J^{nc}.

These in turn depend on the free concentrations of correct and incorrect substrates as well as the enzyme's catalytic efficiency, the k_{cat}/K_M parameter, with each substrate [82]. The ratio of the two k_{cat}/K_M parameters, the normalized accuracy (A), denotes how many correct reactions take place for each incorrect one at equal concentration of correct and incorrect substrates.

$$\frac{J^c}{J^{nc}} = \frac{\left[S^c\right]}{\left[S^{nc}\right]} \cdot \frac{\left(k_{cat}/K_M\right)^c}{\left(k_{cat}/K_M\right)^{nc}} = \frac{\left[S^c\right]}{\left[S^{nc}\right]} \cdot A$$

In living cells the accuracy of translation at each codon therefore depends on the concentrations of correct ternary complex species, the concentrations of incorrect ternary complex species and how well the ribosome can discriminate against the different incorrect ternary complexes. In general, for any codon the concentration of incorrect ternary complexes exceeds the concentration of correct ones by one to two orders of magnitude [83]. Hence, even though the frequency of a *specific* misreading event *in vivo* is on average between 10^{-4} and 10^{-3} the overall error frequency (E) is likely around one order of magnitude higher.

$$E = \frac{J^{nc}}{J^c + J^{nc}} = \frac{1}{1 + \frac{J^c}{J_{nc}}} = \frac{1}{1 + \frac{\sum_i \left[\mathrm{T}_3\right]_i^c \cdot \left(k_{cat}/K_M\right)_i^c}{\sum_i \left[\mathrm{T}_3\right]_i^{nc} \cdot \left(k_{cat}/K_M\right)_i^{nc}}}$$

For any reaction mechanism the normalized accuracy A can be expressed as a function of the elemental rate constants of the partial reactions. For there to be discrimination between two different substrates some of these elemental rate constants have to differ between the two reactions. Differences in the rate constants are due to a difference in the standard free energy between the transition states for correct and incorrect substrates and thus ultimately due to structural differences between the two substrates. It was originally thought that it would be very difficult for enzymes to discriminate between similar substrates as differences in binding free energies were thought to be small [84]. Moreover, these differences define the maximum possible accuracy for the enzyme with that substrate pair and there exists a trade-off between the efficiency of the correct reaction and the accuracy. The maximal accuracy can only be attained when the efficiency of the correct reaction is zero, when both correct and incorrect substrates are allowed to equilibrate with the enzyme [16, 85, 86].

It was independently discovered by John Hopfield and Jacques Ninio in 1974 that enzymes can circumvent these restrictions by so called kinetic proofreading [87, 88]. In proofreading schemes the reaction of interest is coupled to an essentially irreversible reaction with a cosubstrate. The enzyme now gets two chances to reject an incorrect substrate, before and after cleavage of the cosubstrate, and the total accuracy of the whole process can be as high as the product of the individual accuracies of the two steps. This allows for both higher accuracy, as even a small difference between two substrates can be utilized more than once, and higher reaction speed, as each selection step can operate further from equilibrium. For this to work it is essential that the cosubstrate is present far above equilibrium with the coproduct to provide the thermodynamic driving force that keeps the two selection steps separate [89].

The ternary complex of EF-Tu(GTP) and AA-tRNA contains just such a cosubstrate in the form of GTP and this GTP molecule is hydrolyzed during tRNA selection on the ribosome. This made kinetic proofreading a very attractive hypothesis to explain the simultaneously high speed and accuracy of translation *in vivo*. Soon after the discovery of kinetic proofreading it was demonstrated experimentally, using reconstituted *in vitro* translation systems, that it is indeed used by the ribosome during decoding [90, 91]. Decoding on the ribosome is thus split into two steps, the so called initial selection preceding the hydrolysis of GTP by EF-Tu and proofreading selection occuring after GTP hydrolysis but preceding the transfer of the nascent polypeptide chain from the P-site tRNA to the A-site tRNA.

Recently, using an optimized *in vitro* translation system [92] (the same *in vitro* translation system used in all experiments in this thesis) the Ehrenberg group here in Uppsala has been able to study the relative contribution of initial selection and proofreading selection to the overall accuracy of decoding [86, 93, 94]. They were able to calibrate their experiments to replicate both the high accuracy and the distribution of error frequencies between different codons measured *in vivo* [80, 81]. These *in vitro* studies revealed that initial selection is typically more accurate than proofreading selection, by about one order of magnitude, and varies between different codon·anticodon pairs, across three orders of magnitude (10^2 to 10^5). The accuracy of proofreading selection and initial selection correlate except at low initial selection accuracy, where the accuracy of proofreading selection remains high to maintain a high overall accuracy [94]. These *in vitro* and *in vivo* studies demonstrated that most mismatches are effectively discriminated against by the ribosome ($A>10^6$) and that consequently most missense errors occur at specific '*error hot-spot*' codons where the accuracy is low.

The induced fit model of decoding

The mechanism of selection of tRNA by the ribosome has been the subject of a large body of both biochemical and structural work. The currently most popular kinetic model of decoding, sometimes referred to as the '*induced fit*' model, was derived primarily from *in vitro* studies performed in the labs of Wolfgang Wintermeyer and Marina Rodnina.

In the induced fit model ternary complexes first bind to the ribosomal A site independently of the codon displayed on the mRNA, both correct and incorrect ternary complexes have the same association and dissociation rate constants to the ribosome [95-97]. Following binding of ternary complex to the A site a conformational change, named "codon recognition", takes place and the ribosome enters a state where the codon on the mRNA and the anticodon on the tRNA interact. In this state the ribosome can either reject the tRNA by returning to the initial binding state or accept it by triggering GTP hydrolysis by EF-Tu. It is here that the model gets its name, for not only lower rates of return to the initial binding state but also higher rates of GTP hydrolysis were estimated for correct as compared to incorrect tRNA [96, 97]. After GTP hydrolysis higher rates of tRNA accommodation and lower rates of tRNA dissociation were estimated for correct than for incorrect tRNA, implying a second such induced-fit.

In a later paper [97] the authors hypothesize that discrimination between correct and incorrect tRNAs is based exclusively on the differences in the forward rate constants of GTP hydrolysis and tRNA accommodation. The experiments that lead to the induced fit model also lead to the conclusion that the ribosome responds uniformly to different codon·anticodon mismatches [98], in spite of the large variations in error frequencies observed *in vivo* [79-81]. A more recent study using an *in vitro* translation system with more *in vivo* like (higher) rate and accuracy did not observe the small K_M values for GTP hydrolysis with incorrect tRNAs that are a feature of the induced fit model [92]. These studies, as mentioned above, also observed large *in vivo*-like variation in the accuracy for different mismatches [86, 93, 94]. Another study, using single molecule FRET, did not observe the large difference in GTP hydrolysis rates between correct and incorrect tRNAs that gave the induced fit model its name [99].

Structural studies of decoding

In early X-ray crystallographic structures of the 30S subunit an induced fit was observed when an ASL, matching the codon on the mRNA, was bound in the ribosomal A site [100, 101]. Three bases in 16S rRNA, A1492, A1493 and G530 were observed in a different position to the one that they occupy in the

apo ribosome. They had changed their position to interact with the minor groove of the codon·anticodon helix. In particular, the bases A1492 and A1493 had flipped out from h44 to make so called A-minor interactions with the codon·anticodon helix. Such interactions require a conformation close to correct Watson-Crick base-pairing and therefore monitor the sequence complementarity of the codon and the anticodon through the geometry of the resulting helix. Further structural changes in the 30S subunit termed, "domain closure", where the head and shoulder regions of the 30S closed around the A site, were also observed [102]. When ASLs with a single mismatched base compared to the mRNA codon were used, none of these structural changes were observed unless the error-inducing antibiotic paromomycin was also present [102]. It was hypothesized that the energy from the A-minor interactions drives the 30S domain closure [102, 103] and that this in turn could explain the higher rates of GTP hydrolysis and tRNA accommodation for correct compared to incorrect tRNAs.

More recently, high resolution structures of the entire 70S ribosome in complex with several incorrect tRNAs have been solved [104, 105]. In these structures an identical conformation of the ribosome is observed regardless of the sequence complementarity between the anticodon on the tRNA present in the A site and the mRNA. Notably the codon·anticodon helix displays Watson-Crick geometry and the bases A1492, A1493 and G530 occupy identical, flipped out, positions in all of the structures. The observed ribosome conformation corresponds to the domain closure proposed observed in the earlier structures of the 30S subunit with an ASL in the A site. The tRNA molecules in these structures are fully accommodated into the 50S A site and therefore these are snapshots of post-selection states. However, they do suggest that all tRNAs pass through the same states (or at least end up in the same state) as they pass through the decoding reaction. This fully closed state with monitoring bases interacting with the codon·anticodon helix has, based on computational studies, been suggested as the state with the maximum possible discrimination between correct and incorrect tRNAs [106, 107].

Both the structures of the 30S subunit and the 70S ribosome demonstrate that there is an induced fit when the ternary complex binds to the ribosomal A site. The computational studies further demonstrate that the induced conformation is significantly higher in energy for incorrect than for correct tRNAs and therefore should be populated to a much lower extent when an incorrect tRNA is present in the A site. The data in all of these studies are silent on the magnitude of the kinetic rate constants for the relevant reactions. Here it is important to remember that the induced fit demonstrated in these structures, and the notion of induced fit in classical enzymology [82, 108], is distinct from the 'induced fit model' proposed for mRNA decoding by Rodnina and coworkers.

The present work

Methods

The *in vitro* translation system

All experiments in this thesis have been carried out using an *E. coli* based *in vitro* translation system developed here in Uppsala [109]. In this system most reactions in translation take place at *in vivo* like rates. This means that the rate and fidelity of reactions in the system are comparable to best estimates from living *E. coli* [2, 79]. The ribosomes, initiation factors, elongation factors, release factors, ribosome recycling factor, aminoacyl-tRNA synthetases and tRNAs are all purified from *E. coli* cells. Most of the proteins are overexpressed as His_6 tagged versions and purified by nickel affinity chromatography while the ribosomes and tRNAs are purified in their native form directly from wild type cells. mRNAs are produced either by *in vitro* transcription of DNA templates or purchased from companies where they are chemically synthesized. This setup allows for complete control of the composition of any reaction mixture, greatly simplifying experimental design and analysis. The buffer system used in all of the experiments was also developed in Uppsala. This "polymix" buffer was developed to optimize speed and accuracy of *in vitro* poly-Phe synthesis [110]. It contains a mixture of various salts at similar concentrations to what is found in *E. coli* cells as well as the two physiological polyamines spermidine and putrescine. In total the buffer contains 5 mM of Mg^{2+} ions, but in all of our experiments 1 mM GTP, 1 mM ATP and 10 mM PEP are added to provide the system with an energy supply. All of these components chelate Mg^{2+} ions and reduce the free concentration of Mg^{2+} ions to around 1.3 mM [86], close to measurements of the concentration in the *E. coli* cytoplasm [111]. This is of particular importance as both the rate and accuracy of protein synthesis is very sensitive to the Mg^{2+} concentration [44, 86]. To date, this system has been used to study all of the four phases of protein synthesis [44, 51, 92, 112, 113].

Quench-flow

The principle behind the quench-flow method is very simple. A reaction is started by the mixing of two solutions, containing for instance an enzyme and a substrate. Some time later the reaction is stopped (quenched) by the addition

of a quencher, in our case formic acid. The resulting mixture can then be analyzed to determine the amount of reaction product formed by any method of choice. By repeating this procedure for several time points the reaction kinetics can be deduced. In principle this can be done by hand with a pipette and a stopwatch but under *in vivo* like conditions most of the reactions in protein synthesis take place on a timescale of milliseconds so that manual mixing is impossible. Instead a quench-flow instrument is employed that can achieve dead times of 2 – 3 ms. Typically, the quench-flow method is employed to analyze reactions that involve the making or breaking of covalent chemical bonds and requires that the reaction products are stable enough to be analyzed after the quenching of the reaction. In our case the quench-flow method is used to analyze either the formation of peptide bonds or the hydrolysis of GTP to GDP and P_i. To do this we use radioactive substrates, tritium labeled GTP or formyl-methionine, and the amount of reaction products formed are analyzed using an HPLC system with on-line radiation detection. The chief advantages of the quench-flow method are its high time resolution and that any method can be used to analyze the quenched reaction mixtures.

Stopped-flow and fluorescence

The stopped-flow method is conceptually very similar to the quench flow method but here the two solutions are mixed inside an observation cell. The reaction can then be followed in real time using spectroscopic methods of detection. This requires that the reaction taking place changes the optical properties of the reaction mixture. For instance, its absorbance, fluorescence or the amount of light scattered. The strength of the method is that unlike quench flow formation of transient intermediates can easily be studied. The chief drawback is that most reactions do not naturally cause a detectable change in the spectrometric properties of the molecules involved. Therefore, labeling with fluorescent dyes, small organic molecules that are covalently attached to the molecule of interest, is commonly used. Care must be taken that the introduction of the dyes does not alter the properties of the molecules. In addition, the interpretation of fluorescence-based kinetics experiments is often far more complex than for quench-flow methods. In this thesis only one kind of fluorescence-based method has been employed. We have used mRNA molecules labeled at their 3' end with the dye pyrene to follow movement of the mRNA through the ribosome during translocation [114]. This is one of the better characterized fluorescence assays for translocation kinetics in that fluorescence intensities for both the start and endpoint complexes of the reaction have been measured. Due to their versatility fluorescence stopped flow experiments are commonly used in ribosome research.

In such fluorescence experiments changes in the fluorescence intensity of a sample are measured. Fluorescence occurs when a molecule absorbs a photon

of light which causes an electron in the molecule to leave its ground state and enter an excited state. This excited state decays rapidly, typically in a few nanoseconds, and some of these decay events lead to the emission of a photon. As a small amount of heat is also produced the emitted light typically has a longer wavelength than the absorbed light. The fraction of excitation events that lead to emission of a new photon is called the fluorescence quantum yield. The total fluorescence intensity of a sample will depend on the number of fluorescent molecules, the intensity of the excitation light (how many photons are there to be absorbed), the quantum yield of the fluorophore (how many absorption events lead to emission) and the lifetime of the excited state (how often can each fluorophore go through an excitation cycle). Fluorescence methods are incredibly useful for kinetics experiments because both the quantum yield and the excited state lifetime are very sensitive to the immediate surroundings of the fluorescent molecule. In a stopped-flow experiment, where molecules may go through several conformational and compositional states, the fluorescence intensity at a given time is given by the number of molecules in each state, and the quantum yield and fluoresence lifetime of each state. The product of the quantum yield and fluoresence lifetime is often called the "fluorescence parameter" or the "intrinsic fluorescence intensity".

$$F(t) = \sum_i C_i(t) \cdot \overline{F_i}$$

If the fluorescence parameter of each state is known beforehand fluorescence experiments are no more difficult to analyze than experiments using other methods, such as quench-flow, that directly measure the concentrations of products formed. If, as is usually the case, the fluorescence parameters are unknown, it is not possible to directly determine the number of molecules in the different states from the amplitude variation of the fluorescence curve. This can make it very difficult to assign a given estimated rate constant to a specific reaction step. This can lead to some very counter-intuitive situations. For instance, early fast changes in the fluorescence signal can actually report on events taking place late in the sequence of reaction steps and late slow changes can report on events taking place early in the sequence.

Mean time calculations and model building

Mean time calculations have been used throughout all of the papers in this thesis to analyze the results of our kinetics experiments. They offer a simple method to analyze even fairly complex kinetic schemes for which directly solving the associated set of master equations would be a daunting task. To illustrate how mean time calculations work let us consider the simple case of an enzyme that binds to a substrate and converts it into product. Further, let us

assume that the substrate concentration is very large so that we can consider it to be approximately constant during the reaction.

$$E + S \underset{q_a}{\overset{k_a}{\rightleftharpoons}} ES \xrightarrow{k_c} EP$$

Any kinetic scheme can be formalized as a set of differential equations describing the time-dependent probability of the system to be in a specific state, called master equations. At high concentrations of reacting molecules this probability is equivalent to the fractional concentration of each state. For our example scheme above this gives the following system of differential equations for the time-dependent probabilities of finding the enzyme in the various states E, ES and EP.

$$\begin{cases} \dfrac{dP_E(t)}{dt} = -k_a[S]P_E(t) + q_a P_{ES}(t) \\ \dfrac{dP_{ES}(t)}{dt} = -(k_c + q_a)P_{ES}(t) + k_a[S]P_E(t) \\ \dfrac{dP_{EP}(t)}{dt} = k_c P_{ES}(t) \end{cases}$$

For a simple system like this one we could directly solve the differential equations to get the functions $P_E(t)$, but for more complex systems this can be impossible. Instead we can integrate the system with respect to time, from zero to infinite time, and note that such a time integral over the functions $P_E(t)$ results in the mean time, τ_E, that the system spends in the corresponding state.

$$\begin{cases} \displaystyle\int_0^\infty \frac{dP_E(t)}{dt}dt = -k_a[S]\int_0^\infty P_E(t)\,dt + q_a\int_0^\infty P_{ES}(t)\,dt \\ \displaystyle\int_0^\infty \frac{dP_{ES}(t)}{dt}dt = -(k_a + q_a)\int_0^\infty P_{ES}(t)\,dt + k_a[S]\int_0^\infty P_E(t)\,dt \\ \displaystyle\int_0^\infty \frac{dP_{EP}(t)}{dt}dt = k_c\int_0^\infty P_{ES}(t)\,dt \end{cases}$$

This gives us an algebraic equation system rather than a differential equation system. Such systems are generally simple to solve, in our case for the variables τ_E and τ_{ES}.

$$\begin{cases} P_E(\infty) - P_E(0) = -k_a[S]\tau_E + q_a\tau_{ES} \\ P_{ES}(\infty) - P_{ES}(0) = -(k_c + q_a)\tau_{ES} + k_a[S]\tau_E \\ P_{EP}(\infty) - P_{EP}(0) = k_c\tau_{ES} \end{cases}$$

The terms on the left side of the system are the boundary conditions, the probability of finding the system in the given state at infinite time and at zero time. Let us consider the conversion of one unit of substrate into product, so that $P_E(0) = 1$, $P_{EP}(\infty) = 1$ and all of the other initial and final probabilities are zero. This lets us solve for the two mean times τ_E and τ_{ES}.

$$\tau_E = \frac{k_c + q_a}{k_c[S]k_a}$$

$$\tau_{ES} = \frac{1}{k_c}$$

The total time to go from state E to state EP is now the sum of the time spent in all of the steps preceding EP. This is one of the main advantages of working with times rather than rate constants, the fact that times are simply additive.

$$\tau_{tot} = \tau_E + \tau_{ES} = \frac{k_c + q_a}{k_c[S]k_a} + \frac{1}{k_c}$$

The inverse of the expression for the total time gives the apparent rate constant for the process of converting one unit of substrate into product. In our case it readily rearranges into the famous Michaelis-Menten equation.

$$\frac{1}{\tau_{tot}} = \frac{k_c[S]}{\frac{k_c + q_a}{k_a} + [S]} = \frac{k_{cat}[S]}{K_M + [S]}$$

This additive property of the mean times works for any reaction mechanism. In general, for a system of n states the total time required to get to state n from state 1 is

$$\tau_{tot} = \sum_{1}^{n-1} \tau_i = \int_0^\infty \sum_{1}^{n-1} P_i(t)dt = \int_0^\infty \left(P_n(\infty) - P_n(t)\right)dt$$

This means that even without any knowledge of the underlying mechanism the total time can always be estimated simply from the area between a curve of accumulation of the reaction product of interest and the quantity of that

product at infinite time. Since mean time calculations allow for derivation of simple algebraic expressions for how the total time of a process varies with the concentration of substrates or inhibitors they can be used to make quantitative predictions based on a suggested reaction mechanism. If precise measurements of the reaction kinetics are available mean time expressions can be fit directly to experimental data to give estimates of the elemental rate constants.

Fusidic acid and translocation (Paper I)

Early after its discovery it was suggested that fusidic acid might be a *bona fide* translocation inhibitor [115]. However, it was soon shown that it does not inhibit the movement of peptidyl tRNA from the A to the P site, as fusidic acid stalled ribosomes were puromycin reactive [76, 116]. Puromycin is an antibiotic that is commonly used as a substrate analog for peptidyl transfer in biochemical experiments. It enters the PTC of the ribosome and acts as a peptidyl transfer acceptor. This is not possible when the peptidyl-tRNA occupies the A-site, such as before translocation. It was also found that fusidic acid locks EF-G on the ribosome in a long-lived complex but still allows one round of EF-G mediated GTP hydrolysis [117]. In addition, fusidic acid has only very low affinity for either EF-G or the ribosome on their own but high affinity for the complex of the ribosome and EF-G [118]. The conclusion was that fusidic acid binds to EF-G on the ribosome after GTP hydrolysis and translocation and prevents dissociation of the factor, thus preventing the ribosome from receiving a new ternary complex. Consistent with this view a recent pre-steady state kinetics study has shown that fusidic acid does not inhibit the movement of mRNA or the back-rotation of the ribosomal subunits after translocation [32]. A smFRET study, using fluorescent labels on the ribosomal subunits and EF-G, observed rapid back rotation of the ribosome upon EF-G binding in the presence of fusidic acid but that EF-G remained on the unrotated post-translocation ribosome for an extended time (8.4 s) [119].

There are currently four structures of the *T. thermophilus* ribosome-EF-G complex bound with fusidic acid. Two high resolution crystal structures [77, 120] and two medium resolution cryo-EM structures [39, 78] (this was before the recent cryo-EM "resolution revolution" brought on by direct electron detectors, so medium resolution here means around 8 Å). The first crystal structure [77] is of a post-translocation ribosome with unrotated subunits, no head swivel and two classical P/P and E/E tRNAs, though with the L1 stalk closed and contacting the E-site tRNA. EF-G is bound to the GTPase center of the ribosome and domain IV of EF-G extends fully into the ribosomal A site. The fusidic acid binding site is clearly seen near the nucleotide binding pocket of EF-G between domains I, II and III of the protein. One of the two switch loops

(switch I) that interact with the γ-phosphate of the bound nucleotide in the GTP form of the EF-G [121] is disordered. The bound fusidic acid molecule would overlap with the ordered form of switch I observed in structures of ribosome-bound EF-G with non-hydrolysable GTP analogs [73, 120]. This suggests that fusidic acid can bind only after GTP hydrolysis and explains why fusidic acid is unable to bind to ribosome-EF-G complexes prepared with the non-hydrolysable GTP analog GDPCP [118]. Unlike switch I the switch II loop is ordered as in the structures with non-hydrolysable GTP analogs. As switch II is in a different conformation compared to structures of EF-G in solution (believed to be close to the GDP form of the factor) it was suggested that fusidic acid prevents dissociation of EF-G by locking the factor in a GTP-like conformation after GTP hydrolysis. The remaining three structures all show the ribosome in (almost) identical conformation, two of these structures [39, 120] contain only one tRNA molecule, bound in an intermediate state of translocation between the P and E sites. I will not discuss these structures here as the last one, a 7 Å cryo-EM structure [78] has two tRNAs bound in similar intermediate states. This structure has slightly rotated ribosomal subunits but its most striking features are a very large head swivel of 18º and the fact that the two tRNA molecules are in the 'chimeric' hybrid states ap/P and pe/E. This nomenclature indicates that the tRNAs have entered the P and E sites on the 50S subunit and on the 30S body but are still interacting with the A and P sites on the 30S head. Further, the mRNA has moved by almost one codon in relation to the 30S body. The fusidic acid binding site is identical to the crystal structure above. Taken together, these structures suggest that fusidic acid could potentially stabilize more than one state of the EF-G bound ribosome.

Experimental results

To clarify the mechanism of fusidic acid inhibition of EF-G mediated translocation we carried out and analyzed tripeptide formation experiments in the presence of the drug. The resulting tripeptide formation time traces had a characteristic biphasic appearance and could be analyzed in terms of a fast phase, reflecting uninhibited ribosomes, and a slow phase consisting of fusidic acid-inhibited ribosomes. By carrying out several such experiments in parallel with an uninhibited control reaction we could precisely estimate the probability of inhibition (P_i) from the fractional amplitude of the slow phase, and the stalling time (τ_i), from the mean time of the slow phase, at a given fusidic acid concentration. The average elongation cycle time (what would be observed in a steady state experiment), calculated according to $\tau_{avg} = \tau_0 + P_i \cdot \tau_i$, varied non-linearly with the drug concentration. This indicated that the drug bound with high efficiency to a ribosomal state where stalling did not occur. Instead drug-bound ribosomes proceeded unhindered to a downstream state where the actual stalling occurred. From these experiments we could determine K_I parameters for the two drug sensitive states of $K_{I1} = 120 \pm 10$ μM and $K_{I2} = 3.5 \pm$

1.7 mM, showing that drug binding to the first state is far more efficient than subsequent drug rebinding events after dissociation from the second, stalled, state. We could also determine the minimal stalling time, corresponding to a single drug binding event followed by drug dissociation as 8.9 ± 0.6 s, in good agreement with the above mentioned smFRET study done under similar experimental conditions [119]. The different fusidic acid sensitivities of the two states can be due to either differences in the lifetimes of the states or differences in the fusidic acid association rate constant to each state.

Since fusidic acid stalls the ribosome after translocation it should also be possible to form the drug stalled state by binding of EF-G and fusidic acid to post translocation ribosomes rather than by trapping of EF-G after translocation. When carrying out such experiments we noticed that ribosomes stalled in this way had a distinct minimal stalling time of 6.1 ± 0.4 s and that slightly less fusidic acid was required to prolong this stalling through multiple drug binding events prior to EF-G dissociation (K_I = 2.8 ± 0.9 mM). This indicated that fusidic acid can stall the ribosome in two separate states, possibly corresponding to the intermediate state observed by cryo-EM [78] and the fully post-translocational state observed by X-ray crystallography [77]. These results lead to a model where there are three fusidic acid-sensitive states in each elongation cycle (Figure 9). The first of these states is the major drug target but drug binding here does not cause stalling. Rather the ribosome continues unhindered to the second drug sensitive state where it stalls for around 8 seconds. After drug dissociation the ribosome can proceed to another drug sensitive state where drug binding leads to stalling for 6 seconds. It is also possible for EF-G to bind directly to the post translocation ribosome in competition with ternary complex and end up trapped by fusidic acid. This however is a very low probability event.

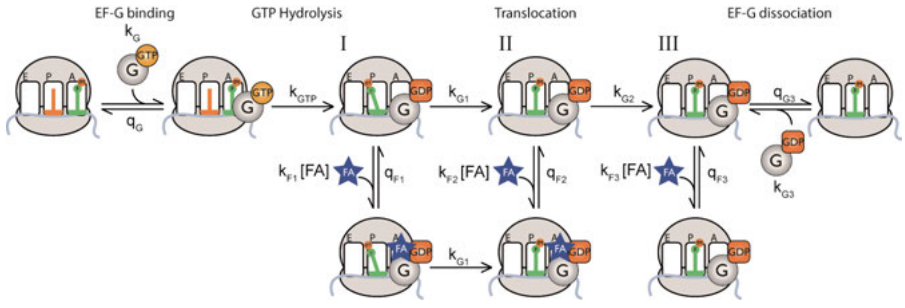

Figure 9. The mechanism of fusidic acid inhibition of translocation. The first drug sensitive state (**I**) occurs early in the translocation process, possibly immediately after GTP hydrolysis. Drug binding to this state does not affect the ability of the ribosome to continue with translocation and drug-bound ribosomes only stall when they reach the second drug sensitive state (**II**). Dissociation of the drug from this state allows progression to the third drug sensitive state (**III**), drug binding here further stalls the ribosome. This last state can also be reached by binding of EF-G and fusidic acid directly to the post-translocation ribosome.

In light of this unexpected complexity of the fusidic acid inhibition mechanism we also carried out mRNA translocation experiments using 3'-pyrene labeled mRNA. We observed no effect on mRNA movement kinetics but did observe that the final fluorescence amplitude (after 5 seconds) varied with the concentration of fusidic acid in a way that implied that fusidic acid-stalled ribosomes yield slightly (~3%) higher fluorescence than fusidic acid-free ribosomes. We did not observe this effect on the fluorescence amplitude when using an mRNA that was one nucleotide shorter at the 3' end, placing the pyrene fluorophore one base closer to the ribosomal P site, though we did observe identical kinetics. That the fusidic acid stalled state yields higher fluorescence than non-stalled states hints at it not being a genuine fully post-translocational state. From this data we could also estimate that 73 ms elapsed between the ribosome becoming translocation competent after peptide bond formation and movement of the mRNA. A further 25 ms elapsed between movement of the mRNA and the ribosome becoming ready to receive a new ternary complex. This suggested that the first, and most sensitive, fusidic acid binding state may occur after GTP hydrolysis by EF-G but before movement of the mRNA.

Structural implications of fusidic acid translocation inhibition

The idea that fusidic acid may bind to EF-G in a pre-translocation state is not incompatible with the two structures of EF-G on the pre-translocation ribosome that exist [74, 122]. In both of these structures the switch regions are disordered and the fusidic acid binding site is accessible. The first structure was determined in the presence of 500 μM fusidic acid however but no clear density was seen for the drug, though the authors could not rule out fusidic acid binding. Whether these structures show authentic pre-translocation states

has been questioned. The first one [74] was captured by blocking translocation with the antibiotic viomycin (we will meet this structure again later). The other [122] used EF-G fused to ribosomal protein L9 and tRNAs with non-reactive aminoacyl analogs in the A and P sites.

Our supposition that the first fusidic acid-stalled state corresponds to the intermediate translocation state observed by cryo-EM [78] is supported by a recent smFRET study [38]. In this study fusidic acid was observed to stall the ribosome in a long-lived state with a large degree of head swivel. Previous single molecule and ensemble FRET studies have shown that fusidic acid stalls the ribosome in a state with unrotated subunits [32, 119] under conditions where the stalling should occur primarily in our first stalling state. It is possible that the methods used did not have the spatial resolution to detect the small degree of 30S body rotation (2.5 º) seen in the cryo-EM structure [78] or that the complex with a full peptidyl tRNA, rather than an aminoacyl tRNA, in the ap/P state has a smaller degree of subunit rotation. The fact that binding of fusidic acid affects the amplitude but not the rate in our translocation assay with a 3' fluorescence labeled mRNA indicates that the mRNA translocation state reported on by this assay is reached in the same time even if reverse head swivel is inhibited by fusidic acid. This indicates that mRNA translocation signal measured by this assay is independent of reverse head swivel, contrary to what has been suggested in the literature based on the similarity in rate of the two processes [40]. But consistent with the fact that the 3' end of the mRNA has moved by almost one entire codon in the crystal structure of a similar fusidic acid stalled intermediate [120].

Fusidic acid inhibition of translocation in the cell

Fusidic acid inhibits two crucial processes in translation, elongation, as described here, and ribosomal recycling. A previous study had suggested that elongation is largely insensitive to fusidic acid (IC_{50} of 200 μM) while recycling is very sensitive (IC_{50} of 0.1 μM) [123]. This contrasted with our results that demonstrated an IC_{50} of 0.6 μM for fusidic acid inhibition of elongation. We were able to show how the experimental design in the previous study greatly reduced sensitivity of their assay to fusidic acid inhibition and led to an artificially large IC_{50} estimate. This prompted reexamination also of fusidic acid inhibition of ribosomal recycling and the Ehrenberg lab has recently published a study that details the inhibition mechanism of fusidic acid in recycling [124]. In short, elongation is the *in vivo* target of fusidic acid and, barring any surprises [125], inhibition of translocation constitutes the greater part of the antimicrobial activity of the drug. The stalling time due to fusidic acid binding is much longer than one elongation cycle, suggesting that when an elongating ribosome becomes stalled by fusidic acid trailing ribosomes on the same mRNA will queue up behind it. This effect would enhance the inhibitory power of the drug as each drug binding event effectively inhibits more than

one ribosome. The magnitude of this enhancing effect on bacterial growth rate is non-trivial to estimate as it depends on the elongation rate for uninhibited ribosomes, the spectrum of initiation rates across cellular ORFs, the length of those ORFs and the abundance of each mRNA. In general, the more ribosomes that are translating an ORF and the closer together they are the greater the enhancement of inhibition by ribosomal queuing. This means that only a small fraction of the ribosomes in a cell need to be inhibited by fusidic acid to have a great effect on the overall translation rate.

Viomycin and translocation (Paper II)

That viomycin inhibits protein synthesis by inhibiting translocation has been known since 1977 [70] and suspected since before then [126]. In their 1977 paper Modolell and Vazquez were able to show that viomycin is capable of interrupting translation of poly-U mRNA in an *E. coli* S100 extract system and that the resulting stalled ribosomes were locked in a state that is not reactive to puromycin. These early studies also showed that viomycin strongly stabilizes binding of tRNAs in the A site. Later studies, using stopped-flow kinetics and fluorescently labeled mRNA or tRNA molecules, have shown that viomycin specifically inhibits movement of the mRNA and tRNAs [28, 114], and that very low (100 nM) concentrations of the drug are required for this effect [127].

Early observations indicated that viomycin binding induces conformational changes across the entire ribosome [128]. The nature of these changes has recently been elucidated by ensemble and single molecule FRET experiments and it has become clear that viomycin stabilizes a specific conformation of the dynamic pre-translocation ribosome. Viomycin-bound ribosomes have rotated subunits [72, 129], tRNAs preferentially in the hybrid state [72], closed L1 stalk and a partly swiveled 30S head [38]. This structure most likely corresponds to one of the suggested extremes of pre-translocation ribosome dynamics [22, 41]. One single molecule FRET study observed multiple long-lived EF-G binding events to such viomycin-stalled ribosomes and suggested that futile GTP hydrolysis by EF-G likely occurs [119], in line with earlier observations that viomycin does not inhibit GTP hydrolysis by EF-G [70]. In both this study and a later single-molecule study [38] the presence of EF-G, and EF-G binding to the ribosome, did not shift the ribosome from the preferred viomycin-bound conformation or affect the dynamics of viomycin-bound ribosomes.

There are currently four structures of the viomycin-bound ribosome, three high resolution crystal structures [71, 73, 130] and one medium resolution

cryo-EM structure [74]. The first crystal structure, of the *T. thermophilus* ribosome with an A-site peptidyl tRNA and a deacylated P-site tRNAs, shows the viomycin binding site between h44 of the 30S subunit and H69 of the 50S subunit. From this structure it is clear that viomycin binds in a pocket in h44 that is formed when the 'monitoring' bases A1492 and A1493 flip out during tRNA selection. It is also clear that drug binding is incompatible with the flipped-in conformation that these bases occupy in the absence of an A-site tRNA. Curiously the ribosome is in a non-rotated conformation in this structure and the two tRNAs are in their A/A and P/P positions. The reason for this is unclear, it may be due to crystal packing or to the use of ribosomes from the thermophile *T. thermophilus* at room temperature. The cryo-EM structure is of an *E. coli* ribosome with peptidyl tRNA in the A site, deacylated tRNA in the P site and with EF-G bound. These ribosomes are in the rotated conformation, the two tRNAs are in the hybrid state (though the A-site tRNA is configured slightly differently from its conformation in other structures), the L1 stalk is closed and the 30S head is slightly swiveled. The resolution is not high enough to determine the atomic details of the viomycin binding pocket but the drug molecule can be clearly seen. The second crystal structure (or set of structures) of the *E. coli* ribosome lacks an A-site tRNA, has a deacylated tRNA in the P site and EF-G, with the non-hydrolysable GTP analog GMPPCP, bound in a post-translocation conformation (it was arrived at in an attempt to trap the EF-G- and RRF-bound ribosome). This set of structures shows viomycin bound in the same binding site in h44 as the earlier crystal structure, but with varying occupancy (judged by the quality of the electron density map) between the different ribosome conformations observed. The third crystal structure also of the *E. coli* ribosome lacks both A-site and P-site tRNAs, is fully rotated and has RF3 bound to the ribosome. Again the viomycin binding site looks the same as in the other structures and the presence of the drug appears to not have altered the overall conformation of the ribosome from that with only RF3, but no viomycin, bound. The presence of the drug did improve the overall resolution of the crystal structure, consistent with results that viomycin suppresses ribosome dynamics [38, 129, 131]. From all of these structures it is unclear how viomycin can have such a large effect on the conformation and dynamics of the entire ribosome.

Experimental results

To understand the effect of viomycin on translocation we carried out and analyzed a large set of tripeptide formation experiments. The kinetics of tripeptide accumulation could be analyzed (like in the case of fusidic acid) in terms of a fast phase and a slow phase. The fraction of viomycin inhibited ribosomes, or the probability of inhibition, at different concentrations of viomycin and EF-G could be estimated from the fractional amplitude of the fast phase compared to an uninhibited control reaction carried out simultaneously. Due to a loss of radioactive signal at long time points, caused by viomycin-induced

read-through of the stop codon of our short ORF, it was not possible to estimate the rate of tripeptide formation on viomycin-bound ribosomes directly from these experiments. Instead this rate was estimated from separate experiments where pre-translocation complexes were pre-equilibrated with viomycin before EF-G was added to the reaction and a truncated mRNA was used to avoid read through.

The fraction of inhibited ribosomes increased hyperbolically with the viomycin concentration and was EF-G concentration dependent such that the higher the EF-G concentration the more viomycin was required to achieve the same inhibition probability. This result is fairly intuitive in that both viomycin and EF-G bind to the pre-translocation ribosome so that lower EF-G concentrations and therefore a lower effective rate of EF-G binding affords viomycin more time to bind. One surprising finding was that when viomycin was pre-equilibrated with the 70S initiation complex no additional drug binding was seen, the expectation being that all ribosomes would have been inhibited already at low viomycin concentration. From this observation we concluded that viomycin binds poorly to the initiation complex and requires an authentic pre-translocation complex, with an A-site tRNA. to which it binds with very high affinity [127]. We were also able to estimate a K_I value from these experiments. This parameter estimates how much viomycin is required for a 50% probability of inhibition at a given EF-G concentration and is therefore unitless (it is effectively a proportionality constant). At our experimental conditions it was 0.55 ± 0.03, indicating that viomycin binds roughly twice as fast as EF-G to the pre-translocation ribosome.

The time required for tripeptide formation on viomycin-inhibited ribosomes increased linearly with the viomycin concentration, indicating that viomycin dissociation can be followed by rebinding events that prolong the stalling. Unlike the probability of inhibition, the linear increase of the stalling time was not EF-G-concentration dependent. This implies that after the first viomycin binding event subsequent drug dissociation and rebinding events occur on an EF-G-bound ribosome complex that is competent to translocate once the drug dissociates. From these experiments the stalling time for a single drug binding event was estimated as 44 ± 1 seconds and the K_I value for drug binding to the EF-G-bound ribosome was estimated as 66 ± 5 μM. The average elongation cycle time, $\tau_{avg} = \tau_0 + P_i \cdot \tau_i$, in the presence of viomycin increased non-linearly with the viomycin concentration, similarly to the behavior with fusidic acid, demonstrating that there is more than one viomycin-sensitive pre-translocational state. From the resulting kinetic model, we could derive an analytical expression for the average elongation cycle time that can be used to estimate IC_{50} values for the drug under different cellular conditions, defined as the drug concentration required to double the average elongation cycle time. For a rapidly growing *E. coli* cell with an elongation cycle time of 50 ms [2, 8] and a

free EF-G concentration of 10 µM [2, 132] only around 6 nM viomycin is required to halve the elongation rate.

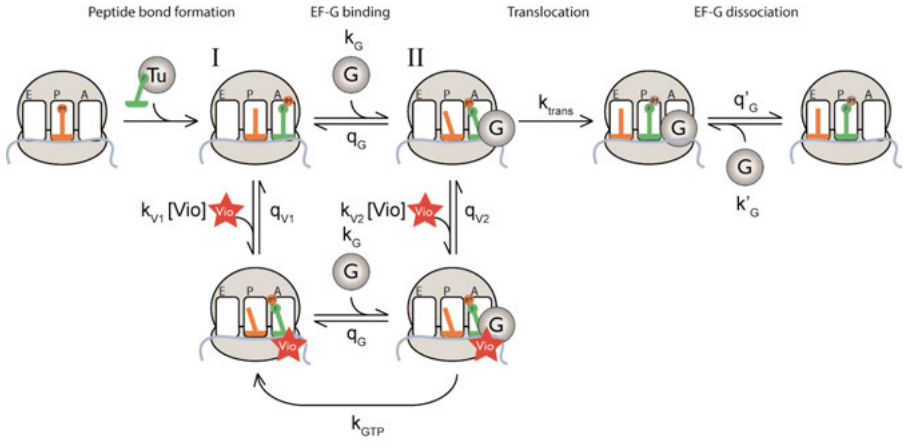

Figure 10. Viomycin inhibition of translocation. Viomycin can bind to the ribosome with high efficiency after a ternary complex has delivered a tRNA to the A-site (**I**). Drug binding to this state does not stall the ribosome but allows EF-G to bind and attempt to translocate bringing the ribosome to the second drug sensitive state (**II**). Drug dissociation from this state leads rapidly to translocation unless very high concentrations of viomycin are present allowing for rapid rebinding. EF-G bound to state **II** is able to hydrolyze GTP and futile cycles of GTP hydrolysis take place.

We also confirmed that binding of EF-G to viomycin-bound ribosomes does cause futile rounds of GTP hydrolysis by EF-G, as suggested earlier [119]. From our data we could calculate a dwell time for EF-G on the stalled ribosome of 270 ± 15 ms. This number agrees well with the dwell time estimate from based on smFRET measurements under experimental conditions similar to ours [119]. Our measurements also indicated that EF-G binds to the viomycin-stalled ribosome with very high affinity, rationalizing why there is no EF-G concentration dependence for the prolongation of the stalling time due to viomycin rebinding after the first dissociation event. This futile cycling of EF-G increases the energy cost of translation. At the viomycin concentration of 6 nM mentioned above an average elongation cycle consumes around 10% more GTP molecules than in the absence of viomycin.

Structural implications of viomycin translocation inhibition

From our data it is very clear that viomycin has only very low affinity for ribosomes with an empty A site. Together with previous observations from others [127, 133], it appears that the presence of a tRNA in the A site increases viomycin affinity for the ribosome by at least two orders of magnitude. This is reasonable considering that the viomycin binding site is in the pocket formed when the monitoring bases A1492 and A1493 flip out to interact with

the codon·anticodon minihelix (more on this later in the section about viomycin and translational accuracy). It then seems odd that there are two crystal structures of ribosomes lacking A-site tRNA but with viomycin bound [73, 130]. Here it should be considered that very high concentrations (much higher than in our study) of viomycin were used in the crystallization buffers, 500 μM in [73] and 1.5 mM in [130] which could certainly drive drug binding also in the absence of an A-site tRNA.

Our result that prolongation of the stalling time by repeated viomycin binding events occurs primarily on an EF-G-bound ribosome agrees with the high affinity of EF-G for stalled ribosomes observed previously [119], and by us. The fact that the prolongation of the stalling time is independent of the EF-G concentration indicates that these EF-G-bound ribosomes are able to translocate within a short time after drug dissociation. Notably, translocation does not require dissociation of the bound EF-G and association of a fresh EF-G before drug rebinding. This implies that the EF-G-bound pre-translocation ribosome observed by cryo-EM [74] is either an on-pathway translocation intermediate or can rapidly reorganize itself into one upon dissociation of viomycin. Dissociation of EF-G from the stalled ribosome requires progression through several conformational states with similar lifetime [119], during one of which GTP hydrolysis occurs. In the cryo-EM structure [74] the resolution was unfortunately not high enough to gauge the phosphorylation state of the nucleotide on EF-G. This leaves open two possibilities: either GTP hydrolysis occurs late in the sequence of events and EF-G dissociates rapidly afterwards, or it occurs early but release of inorganic phosphate does not occur until later and viomycin dissociation is followed by translocation mediated by EF-G with bound GDP and P_i. Such translocation has recently been inferred to be surprisingly efficient based on the high translocation rates observed with GDP and phosphate analogs [34].

Viomycin translocation inhibition in the cell

The calculated IC_{50} for viomycin inhibition under cellular conditions is *very* small and the stalling time of 44 s is very much longer than an average elongation cycle. The calculated IC_{50} corresponds to a free viomycin concentration under the assumption that viomycin is present in excess over translating ribosomes and that each ribosome works as a free floating enzyme. Both are unlikely in a living bacterium. Viomycin has very high affinity for its target and the concentration of elongating ribosomes in the cell is very high. This implies that almost all viomycin molecules present in a bacterial cell would be ribosome-bound at steady-state. Like for fusidic acid, the stalling time of 44 seconds is much longer than an average elongation cycle for a drug free ribosome, therefore viomycin binding likely causes ribosome traffic jams as trailing ribosomes end up stalled behind the viomycin-bound ribosome. The same considerations as for fusidic acid apply also to viomycin, but with a much longer

stalling time, 44 s versus 8 s, queueing is likely an even bigger factor for viomycin inhibition.

Viomycin and decoding (Paper III)

That viomycin causes misreading of the genetic code was established already in the 1980s [69], using a poly-U translating *in vitro* system. However, another earlier study [134] observed no stimulation of missense errors by viomycin. In addition, miscoding was not observed in *in vitro* full length protein synthesis [135], something that is observed for the known error-inducing aminoglycoside antibiotics [136]. Hence, even though viomycin causes miscoding (we had also observed viomycin-induced misreading in our translocation experiments, notably by a tRNA with two nucleotides mismatched to the mRNA), the role of this miscoding in the antimicrobial activity of viomycin was unclear.

Experimental results

We measured how viomycin present at different concentrations affected the k_{cat}/K_M of GTP hydrolysis and peptide bond formation for $tRNA^{Phe}$-containing ternary complexes reading both correct and incorrect codons. We found that viomycin increased the k_{cat}/K_M of both GTP hydrolysis and peptide bond formation for reading of the near-cognate codon CUC but had no effect whatsoever on $tRNA^{Phe}$ reading its cognate codon UUC. The k_{cat}/K_M of GTP hydrolysis for the incorrect reaction was viomycin concentration dependent, with no sign of saturation, up to a viomycin concentration of 1 mM. The k_{cat}/K_M of peptide bond formation for the incorrect reaction had an identical viomycin concentration dependence. At all tested viomycin concentrations the k_{cat}/K_M of GTP hydrolysis and the k_{cat}/K_M of peptide bond formation were the same, indicating that proofreading selection is completely absent on viomycin-bound ribosomes.

From these experimental observations we constructed a kinetic model for initial selection that contained two ribosomal states before GTP hydrolysis. In this model, when ternary complex first binds to the A site the codon·anticodon interaction is either unformed or not monitored by the ribosome and the selectivity between correct and incorrect tRNAs is very small. Both the dissociation rate constant for the ternary complex from this state and the rate constant for moving forward in the selection process are independent of the complementarity between the codon and the anticodon (though not necessarily independent of the nature of the tRNA itself). Viomycin either does not bind to this state or has no effect if it does. The smallest accuracy that we observe in the presence of viomycin is about four, but since drug binding is far from saturation

the residual selectivity of any drug-immune states can only be at most two-fold.

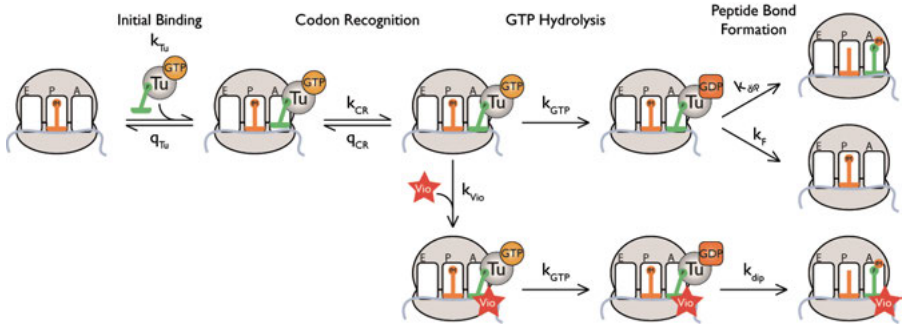

Figure 11. Mechanism of viomycin inhibition of mRNA decoding. Viomycin binds only after the monitoring bases A1492 and A1493 have flipped out during codon recognition. Viomycin-bound ribosomes lose all ability to discriminate between different tRNAs and pass both initial selection and proofreading selection.

Moving forward from this initial binding state the tRNA arrives at a state where the codon·anticodon interaction does matter. Here correct tRNAs proceed forward to GTP hydrolysis with high probability and incorrect tRNAs are rejected and return to the initial binding state with high probability. It is to this selective state that viomycin binds and affects the selection process. Drug-bound ribosomes are rendered incapable of rejecting the tRNA and will proceed forward with both GTP hydrolysis and peptide bond formation. Using this model (and the assumption that any viomycin-insensitive states are non-selective), we could estimate the probability of drug binding during initial selection. This let us define a K_I value as the viomycin concentration required for a 50% probability of drug binding. For $tRNA^{Phe}$ reading four separate near-cognate codons, CUC, AUC, UAC and UUA (the underlined base is different from the cognate codon UUC) we observed a clear correlation between K_I and the accuracy of initial selection.

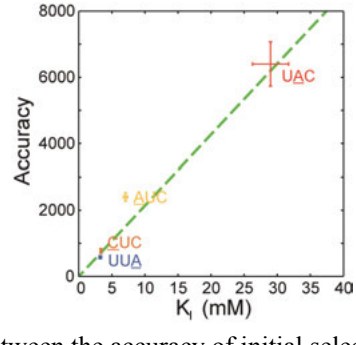

Figure 12. Correlation between the accuracy of initial selection and viomycin sensitivity for the four mismatches CUC, AUC, UAC and UUA.

The concentration of viomycin required for a certain probability of binding during initial selection is proportional to both the lifetime of the drug-sensitive state and the binding rate constant of the drug.

$$K_I = \frac{1}{k_{Vio}} \cdot \frac{q_{CR}}{\left(1 + \frac{k_{CR}}{q_{Tu}}\right)}$$

Interestingly the K_I value is insensitive to the size of the rate constant of GTP hydrolysis, whereas the accuracy is not. This is because the lifetime of the drug sensitive state is proportional to the sum of the rates of GTP hydrolysis and tRNA rejection (where k_{GTP} can be neglected as it is much smaller than q_{CR}) while the accuracy is proportional to their ratio. Hence, strong correlation between the accuracy of initial selection for different codon·anticodon pairings and the viomycin K_I for those pairings implies that the variation in accuracy derives entirely from variation of the rate of tRNA rejection while the GTP hydrolysis rate remains constant. It is then not far-fetched to suggest, in contradiction to the '*induced fit*' model described above, that accuracy in translation is primarily achieved through more rapid rejection rates of mismatched tRNAs rather than slower acceptance rates.

Further discussion of the induced fit model

As our experimental results contradict the induced fit model it is important to consider how well supported this model is by the available experimental data. As mentioned above several more recent studies have failed to observe many of the key predictions of the induced fit model, namely small K_M values for incorrect reactions [92] and large differences in GTP hydrolysis rates with correct and incorrect tRNAs [99]. However perhaps more importantly the notion of faster GTP hydrolysis for correct reactions is not well supported by the data presented in the original induced fit papers themselves [96, 97].

In these papers the authors note that the global fit software used fails to arrive at a singular solution (parameter estimate) for their experimental data. They go on to mention that in order to arrive at definite parameters values they had to provide the software with additional data, to "fix" certain parameters. The authors carried out a chase experiment (Figure 13) to directly estimate the rejection rate of near-cognate tRNA (called q_{CR} throughout this thesis and k_{-2} in [96] and [97]). The authors equilibrated ribosomes programmed with poly-U mRNA with ternary complexes containing proflavin labeled $tRNA_2^{Leu}$ and either the non-hydrolyzable GTP analog GDPNP [96] or the GTPase-deficient EF-Tu mutant H84A [97]. Since these ternary complexes are incapable of carrying out GTP hydrolysis initial selection was stalled at some prior point. The pre-equilibrated ribosome complexes were then mixed with fully functional

ternary complexes containing GTP and the dissociation of the near-cognate ternary complex from the ribosome could be followed as a decrease of the proflavin fluorescence. The authors estimated the dissociation rate by fitting of a single exponential function to the data and took this estimated rate as q_{CR} (k_{-2} in [96] and [97]).

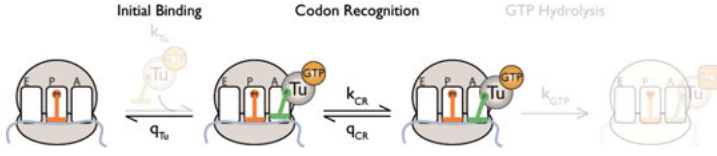

Figure 13. Schematic view of the chase experiment to determine q_{CR} discussed in this section. Ribosomes bound by ternary complex that are unable to hydrolyze GTP are in equilibrium between two states leading to complex dissociation kinetics.

However, the rate estimated from such an experiment is only equivalent to q_{CR} in a few special cases. In the general case the mean time (inverse of the rate) for ternary complex dissociation is given by the following expression.

$$\tau_{chase} = \frac{1}{q_{Tu}} + \frac{f_2}{q_{CR}} + \frac{k_{CR}}{q_{Tu} q_{CR}} \qquad f_2 = \frac{k_{CR}}{k_{CR} + q_{CR}}$$

In both [96] and [97] the rate estimated from the chase experiment is identical (within the experimental precision) to the rate of ternary complex dissociation from the initial binding state estimated from another fluorescence experiment. This is only possible if essentially all of the ribosomes are in the initial binding state when the experiment begins, that is if q_{CR} is much larger than k_{CR}. The results of these chase experiments are therefore in contradiction to the parameter values presented in [96] and [97], yet using these results to fix the size of q_{CR} was crucial to estimating those very parameters by global fitting. Thus, the model and the parameter values presented in [96] and [97] cannot be used to reconstruct the experimental data upon which they were based. The conclusion that the rate of GTP hydrolysis is smaller for incorrect than for correct reactions on the ribosome is therefore not supported by the data. In fact the data are entirely ambivalent with regards to the size of k_{GTP} with correct and incorrect substrates.

Structural implications of the viomycin error-induction mechanism

As viomycin binds in a pocket formed when the bases A1492 and A1493 flip out of helix 44 to engage with the codon·anticodon helix, the fact that viomycin causes missense errors implies that these bases do engage also with mismatched codon·anticodon helices. In the original crystal structures of the ribosome [4, 101, 137, 138] these bases were highly disordered (judged by high B-factors) when no tRNA was present in the A site. In addition, several NMR

[139, 140] and computational [141, 142] studies have indicated that these bases are dynamic in the absence of tRNA and suggested that tRNA binding might shift the equilibrium towards the flipped-out state. The correlation we observed between the accuracy of initial selection and the viomycin sensitivity implies that the better the ribosome discriminates against a certain mismatch the shorter is the time that the viomycin binding site remains accessible. This leads to a model where upon entry of a tRNA into the A site the bases A1492 and A1493 rapidly flip out (or are already flipped-out) from h44 and engage the codon·anticodon helix. If the codon and the anticodon match the resulting state is low in energy and therefore stable, if not it is high in energy and therefore unstable, as suggested from computational studies [106, 107]. It is tempting to identify this state with the fully closed 70S structure observed with mismatched tRNAs [104, 105], but with the tRNA in the bent A/T conformation rather than the A/A conformation. Such a structure has been observed for tRNAs with a third position mismatch [143]. This observation was explained by A1492 and A1493 not monitoring third position mismatches, even though third position mismatches can be just as accurate as first or second position ones [93]. In addition, a computational study has suggested that third position mismatches could be sensed through alteration of the minor groove geometry of the first two base pairs [144]. However, full domain closure is not necessary to explain our observations, it is enough that A1492 and A1493 flip out to open the viomycin binding site, and that the time they spend flipped out depends on the nature of the codon·anticodon interaction.

Viomycin-induced errors in the cell

Our results allowed us to derive a model for the frequency and distribution of viomycin-induced missense errors. Unfortunately, quantitative predictions from this model require knowledge of the free concentrations of all tRNA species in the cell as well as the K_I values for all possible mismatches.

$$E^{Vio} = \sum_i \frac{[T_3]_i^{nc}}{[T_3]_{tot}} \cdot \frac{[Vio]}{[Vio] + K_{Ii}}$$

Qualitatively this model predicts that the frequency of viomycin-induced errors will be maximal for codons where there is a high concentration of incorrect ternary complexes, a low concentration of correct ones, and a small accuracy of initial selection. These are the same conditions that cause the naturally occurring error hot-spots mentioned earlier [81, 93], and as viomycin completely disables proofreading selection it is unable to carry out its hypothesized function of neutralizing these hot spots [94]. Error hot spots in initial selection are probably selected against in important positions in protein coding genes, implying that most viomycin-induced errors have a small effect on fitness. However, viomycin will not only increase the frequency of errors but

also change their distribution, by changing the relative accuracy of all codons (by disabling proofreading). This change in error distribution likely serves to increase the effect of the caused errors on the cell at least a little bit. This assumes that accuracy is so important to the cell that the accuracy of a given codon position is proportional to the fitness cost of missense errors at that position, which is not necessarily the case. It is hard to escape the idea that error induction by viomycin is probably more like a side-effect of its translocation inhibition, especially given how incredibly sensitive translocation is to viomycin. Misreading may be important for the side effects caused by viomycin as eukaryotic and mitochondrial ribosomes are much less sensitive than bacterial ribosomes to translocation inhibition by viomycin but appear to be sensitive to its error induction activity [135].

ΔTlyA mediated viomycin resistance (Paper IV)

Antibiotic resistance is a significant public health issue both in the developing world and in first world countries. Tuberculosis treatment is almost perfectly designed to generate resistance mutations. The treatment courses are long, typically 6 – 12 months and three separate antibiotics must be taken in unison. When *M. tuberculosis* develops resistance to first line drugs so-called second line drugs are used. One of these is capreomycin, a drug from the same family as viomycin, that binds to the same site on the ribosome and works in the same fashion. In 2005 it was shown that *M. tuberculosis* can develop resistance to capreomycin and viomycin by inactivation of the gene *tlyA* and that such inactivation was common in clinical isolates [145]. The following year it was shown that the *tlyA* gene product is an rRNA methyltransferase that methylates the 2'-OH of two rRNA bases, C1406 in the 16S rRNA and C1920 in the 23S rRNA [146]. Loss of the two rRNA methylations is what confers resistance to viomycin. Not all bacteria have a TlyA enzyme. In particular *E. coli* does not and therefore naturally lacks the two rRNA methylations. Heterologous expression of the enzyme in *E. coli* leads to both rRNA methylation and increased susceptibility to viomycin [146]. The resistance gained by *tlyA* inactivation is not high, minimum inhibitory concentrations (MIC) determined by plating assays only increase four to eight fold. But under laboratory conditions the loss of the methylations in mycobacteria or the introduction of them in *E. coli* has no effect on bacterial growth rate [147].

No high resolution structures of mycobacterial ribosomes exist so it is not clear what structural effects the methylation of C1409 and C1920 has. The two nucleotides are about 20 Å apart in both the classical and rotated states of the ribosome. Structural modeling based on the *T. thermophilus* ribosome with viomycin bound [71] indicates that the methylated nucleotides are located in the drug binding pocket on the opposite side of the bound viomycin molecule

from the A-site tRNA [147]. In the absence of structural evidence it is unclear whether the methylations make direct contact with viomycin or if they cause remodeling of the drug binding pocket.

Resistance mutations are generally poorly characterized biochemically and several studies suggest that the link between changes in biochemical inhibition and physiological resistance may be complex [148, 149]. Since we have developed mechanistic models for the two modes of action of viomycin we decided to investigate what effect the presence of TlyA mediated rRNA methylations has on viomycin inhibition.

Experimental results

To purify methylated *E. coli* ribosomes, we took advantage of the fact that heterologous expression of the *M. smegmatis* TlyA enzyme in *E. coli* leads to methylation of C1409 and C1920. We then carried out the same experiments as in paper II and III to assess the changes in viomycin inhibition of translocation and translational fidelity. In agreement with the small effects of the rRNA methylations on bacterial fitness [147] neither the kinetics of GTP hydrolysis by EF-Tu or tripeptide formation differed between methylated and WT ribosomes. Nor did the accuracy of initial selection. For all of the tripeptide formation experiments we used a 3' truncated mRNA to avoid viomycin-mediated read-through. This simplified the data analysis but lead to slower tripeptide formation on uninhibited ribosomes. Viomycin inhibition of tripeptide formation was unaffected by the mRNA truncation. Viomycin inhibition of translocation (Figure 10) was affected in multiple ways by introduction of the rRNA methylations. Viomycin competed slightly better with EF-G for binding to the pre-translocation ribosome, K_{I1} was reduced from 0.55 ± 0.03 with WT *E. coli* ribosomes to 0.33 ± 0.013 with TlyA+ ribosomes. The sensitivity of the EF-G-bound ribosome was drastically reduced, K_{I2} changed from 66 ± 5 μM with WT ribosomes to 800 ± 200 μM with methylated ribosomes. The stalling time increased from 44 ± 1 s with WT ribosomes to 111 ± 2.5 s with methylated ribosomes. Taken together these effects cause a drop in the IC_{50} of translocation inhibition from 6 nM for WT ribosomes to 1.5 nM for TlyA+ ribosomes under *in vivo* like conditions. This fourfold change is suggestively close to the changes in MIC observed in previous studies [145-147].

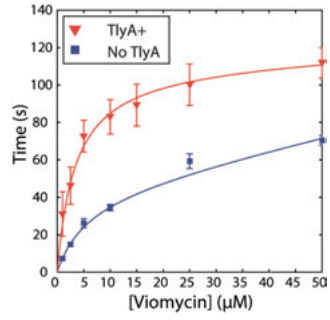

Figure 14. Average elongation cycle time for TlyA+ and WT ribosomes in the presence of different concentrations of viomycin. The average time on TlyA+ ribosomes grows roughly four fold faster at low drug concentrations.

Introduction of the methylations increased the viomycin sensitivity of initial selection by little more than two fold. K_I for $tRNA^{Phe}$ reading the near-cognate codon UUA changed from 3.25 ± 0.2 mM with WT ribosomes to 1.3 ± 0.2 mM with methylated ribosomes. This is likely not due to an extended lifetime of the drug sensitive state as that should lead to lower accuracy of initial selection in the absence of the drug, something that was not observed. These numbers indicate that introduction of the methylations not only stabilizes drug binding by reducing the drug dissociation rate by about 2.5 fold but also either extends the lifetime of the drug sensitive states or increases the association rate constant for viomycin to these states.

The extended residence time of viomycin on TlyA methylated ribosomes is likely due to stabilizing interactions made with the drug either by the methyl groups themselves or by the methylated nucleotides if the presence of the methyl group changes their orientation. A full explanation of this effect will have to await a high resolution structure of a methylated ribosome, preferably bound by viomycin. The increase in the efficiency of viomycin binding points to remodeling of the viomycin binding site, either through local changes to make it more open or by changing the overall conformation of the ribosome. The effects of viomycin itself shows that alterations in this region have the potential to alter dynamics across the entire ribosome.

ΔTlyA mediated resistance in the cell

The close correspondence between the magnitude of the biochemical and physiological effects of the TlyA methylations indicates that the resistance mechanism is fairly straightforward and is probably caused by drug-target interactions rather than by ancillary effects. As discussed above the IC_{50} approximation for translocation inhibition is probably not entirely valid for viomycin under cellular conditions and most of the increased drug sensitivity likely derives from the increased drug residence time. The even longer residence time on methylated ribosomes will cause even more severe queueing of ribosomes

on mRNAs. It is also important to remember that MIC values are not exact measurements of drug sensitivity but rather imprecise approximations, the biochemical effects of the methylations would be better compared to the effect of different concentrations of viomycin on steady-state growth rates.

Conclusions and future outlook

The experiments in this thesis were all aimed at the same goal, to characterize ribosome targeting antibiotics as what they are – enzyme inhibitors. To derive their mechanisms of action and to precisely determine the numerical values of the parameters that govern their inhibitory action. And to do this under reaction conditions as close as possible to those in a living cell so that our results could be used to understand how these molecules affect not just the ribosome but cell physiology as well. What we found in papers I, II and III was that for the two antibiotics we studied, fusidic acid and viomycin, the inhibition mechanisms were unexpectedly complex. Both drugs are able to bind to multiple ribosomal states, and do so with different efficiency. Fusidic acid is even able to stall the ribosome in two different conformations. One curious discovery was that for both drugs the ribosomal state that the drug is most likely to bind to during translation is *not* the state where the drug-bound ribosome actually stalls. That is, the major drug target is distinct from the structure that is stabilized by the drug. If this feature is general it has significant implications for drug design in that structures determined in the presence of a drug may not reflect the state of the drug target when drug binding actually occurs.

The effect of the two rRNA methylations studied in paper IV shows that even small differences in ribosome structure can have large effects on antibiotic inhibition. Our experiments were carried out in an *in vitro* system based on *E. coli* ribosomes and translation factors. It is entirely possible that the two most significant target pathogens for fusidic acid and viomycin, *S. aureus* and *M. tuberculosis* respond differently to the drugs, certainly the exact sizes of the inhibition parameters will differ. Our lab is currently developing a mycobacteria-based *in vitro* translation system. This system is based on *M. smegmatis* rather than *M. tuberculosis* but it is far closer to the clinically relevant target for a large set of ribosome targeting antibiotics than *E. coli*. In the same vein a high resolution structure of the *S. aureus* 50S subunit was recently published [150] and structures of the 70S particle have been presented. High resolution structures of *M. smegmatis* ribosomes are under development by several labs, possibly even in complex with a familiar antibiotic.

The logical next step to extend our studies is to attempt to truly link the biochemical mechanisms of the drugs to their physiological effects. This will re-

quire computer modelling efforts and measurements of global translation using methods such as ribosome profiling. Modeling is helped by the fact that the ribosome is an incredibly important part of the cell and that the growth rate can often be directly related to the rate of translation [151]. However, in a living cell also regulation must be taken into account [152], bacteria do their best to fight the inhibitory effects of an antibiotic even without resistance mutations. To make matters even more complicated recent studies using ribosome profiling have discovered that several well characterized ribosome-targeting antibiotics have unexpected effects in living cells that depend on the mRNA sequence being translated [153, 154]. While it is not clear that the drugs studied here would have such context dependent effects it is always a possibility. Luckily, given a little time such things can always be characterized biochemically.

Sammanfattning på svenska

Den här avhandlingen handlar om antibiotika. Mer specifikt handlar den om hur antibiotika fungerar inne i de otursamma bakterieceller som råkat på den. Hur den inhiberar olika funktioner inne i cellerna så att de inte klarar av att växa och föröka sig. Antibiotika är en viktig del av det moderna samhället, utan dessa läkemedel skulle många behandlingar, även för andra saker än infektionssjukdomar, som är rutin idag vara omöjliga att genomföra. Jag har studerat två olika antibiotika: viomycin och fusidinsyra. Både viomycin och fusidinsyra attackerar bakteriernas ribosomer. Ribosomen är den molekylära maskin i cellen, både i bakterier och i djur som giraffer och människor, som tillverkar alla cellens proteiner. Proteinerna i sin tur gör nästan allt i cellen, de kopierar cellens DNA, skickar signaler inne i cellen för att koordinera dess olika delar, fungerar som sensorer som känner av cellens omgivning och så vidare. Med andra ord, om cellens ribosomer slutar fungera eller fungerar sämre, t.ex. tillverkar proteiner i långsammare takt så får det allvarliga konsekvenser.

Ribosomen tillverkar inte proteiner som den själv känner för utan tar sina order av cellens genom, de DNA molekyler där cellens gener lagras. DNA skrivs av, *transkriberas*, av proteiner kallade RNA polymeraser. Detta skapar ett så kallat budbärar RNA (mRNA). Ribosomen stegar längs med mRNAet och översätter sekvensen av nukleobaser till en sekvens av aminosyror enligt den så kallade genetiska koden. Att det här fungerar över huvud taget är egentligen ganska fantastiskt, ribosomen är en otroligt komplicerad maskin med hundratals ”rörliga delar” och den är inte mer än 20 nm i diameter, ca 5000 gånger mindre än tjockleken på ett människligt hårstrå. Att ribosomen kan lösa sin uppgift både snabbt och med stor noggrannhet är mycket viktigt för cellen. Ju snabbare cellen kan tillverka rätt proteiner desto snabbare kan den föröka sig och reagera på förändringar i sin omvärld.

Varken viomycin eller fusidinsyra är i dagens läge särskilt viktiga antibiotika, de används mest mot ovanliga infektioner orsakade av bakterier som redan utvecklat resistens mot andra antibiotika. Viomycin används förresten nästan inte alls längre men den brukade användas mot tuberkulos. Numera är den dock ersatt av den liknande antibiotikan capreomycin. Antibiotikaresistens är dock ett växande problem och fler och fler gamla antibiotika som viomycin plockas fram ur förråden för att behandla resistenta infektioner. Men den här

avhandlingen handlar egentligen inte om sjukdomar eller behandlingar, den handlar om biokemi.

Målet med studierna som utgör den här avhandlingen var att försöka bestämma hur antibiotika egentligen fungerar. Hur mycket viomycin behövs det till exempel för att få en ribosom att tillverkar proteiner hälften så fort? Trots att viomycin upptäcktes redan 1951 var det ingen som kunde svara på den frågan innan studierna i den här avhandlingen. I papper I studerade vi mekanismen för hur antibiotikan fusidinsyra inhiberar translokeringen, ribosomens rörelse längs med mRNAet. Innan vår studie var det känt att fusidinsyra binder till proteinet EF-G på ribosomen och låser fast det så att det blockerar ribosomen och hindrar den från att fortsätta längs mRNAet. Vi kunde visa att fusidinsyrans mekanism är betydligt mer komplicerad än så. Fusidinsyra kan binda till ribosomen vid tre olika tillfällen under varje steg den tar längs med mRNAet (och den behöver ta hundratals steg för att tillverka ett enda protein). Vidare visade vi att fusdinsyra låser fast ribosomen i hela sex sekunder. Det kanske inte låter som så länge men då bör man tänka på att ribosomen vanligtvis tar nästan 20 steg i sekunden. Så för en ribosom är sex sekunder en väldigt lång tid.

I papper II och III studerade vi hur viomycin dels hindrar ribosomen att röra sig längs med mRNAet och dels hur viomycin kan få ribosomen att läsa den genetiska koden fel och välja fel aminosyra. I papper II kunde vi visa att viomycin låser fast ribosomen i hela 44 sekunder, till och med längre än fusidinsyra. Dessutom krävdes mycket mindre viomycin (än fusidinsyra) för att få samma effekt. I papper III kunde vi visa att även om viomycin får ribosomen att läsa fel så är det inte så alvarligt för cellen, i alla fall inte i jämförelse med hur bra viomycin är på att hindra ribosomen från att röra sig. Men vi kunde även visa att sättet som viomycin fungerar på betyder att några tidigare publikationer om hur ribosomen kan vara så noggrann inte kan vara helt korrekta.

I papper III studerade vi en resistensmutation mot viomycin. Vi kunde visa att om en bakterie inte har den mutationen så blir ribosomen fastlåst av viomycin i 110 sekunder och dessutom så krävs ännu mindre viomycin för att få samma effekt som tidigare. Den här resistensmutationen är väldigt vanlig i tuberkulosinfektioner så förståelse för hur den fungerar kan kanske vara bra för att utveckla nya antibiotika som den inte rår på. Sammantaget har våra studier visat att antibiotika som angriper ribosomen är mycket mer komplicerade än vad som tidigare trots och det kan vara på sin plats att omvärdera några av de metoder som används för att försöka utveckla nya antibiotika.

Acknowledgements

To my supervisor **Suparna**, thank you for allowing me to work in your lab, for your energy, your enthusiasm, your kindness, encouragement, inspiration, support and guidance. If it was not for you I would not be a scientist today.

My co-supervisor **Måns**, I have learnt an enormous amount from you throughout the years, I think at this point I might even be able to pass that exam in Biophysical Chemistry…

Anneli my lab buddy! Thank you for all of the discussions over the years, both about science and non-science. Thank you for being there for me when science was at its darkest. I don't think I would have made it through on my own. And of course thank you for the all-important *transference*!

Mike thank you for keeping the HPLCs in running order and for explaining to me why the data analysis I spent an entire Christmas holiday on was totally wrong.

Chandu and **Ravi**. Thank you for being my office mates for six years and for helping me when I first started in the lab. And thank you for all of the encouragement and support and for sharing the burden of ribosome preps. My time in the lab would have been much less fun without you guys there.

Ray thank you for making all of the components, for being a good person, and for being the only adult in the room most of the time.

Thank you **Rasa** and **Chang-Il** and an extra thanks to **Ravi** and **Anneli** for proofreading the thesis. Thank you **Petar** for being just annoying enough to be funny, most of the time. And thanks to all of the other people in D9:2 that make it the special place that it is, **Liang**, **Yanhong**, **Kaweng**, **Josefine**, **Jinfan**, **Jingji**, **Gabriele**, **Harriet**, **Onur**, **Marek**, **Kristin**, and many others!

To my parents. Thank you for giving me the best start in life anyone could hope for, for your continued support and love. And for reminding me about my sibling's birthdays.

To my brother and sister for making me feel old. Or young, now that Annika has a son, and for reminding me about our parent's birthdays.

To my close friends **Oscar**, **Christer** and **Beatrice**, thank you for all of the good conversations, the support, the encouragement and in some cases the "encouragement".

To my lovely **Volance**. Thank you for the support, the love, the encouragement, the debates, the silliness and the rage. *Ik hou zoveel van je*. Osh!

References

1. Russell, J.B. and G.M. Cook, *Energetics of bacterial growth: balance of anabolic and catabolic reactions.* Microbiol Rev, 1995. **59**(1): p. 48-62.
2. Bremer H, D.P., *Modulation of chemical composition and other parameters of the cell by growth rate*, in *Escherichia coli and Salmonella*, N. FC, Editor. 1996, Am Soc Microbiol: Washington DC. p. 1553-1569.
3. Rheinberger, H.J., H. Sternbach, and K.H. Nierhaus, *Three tRNA binding sites on Escherichia coli ribosomes.* Proc Natl Acad Sci U S A, 1981. **78**(9): p. 5310-4.
4. Wimberly, B.T., et al., *Structure of the 30S ribosomal subunit.* Nature, 2000. **407**(6802): p. 327-39.
5. Ban, N., et al., *The complete atomic structure of the large ribosomal subunit at 2.4 A resolution.* Science, 2000. **289**(5481): p. 905-20.
6. Schluenzen, F., et al., *Structure of functionally activated small ribosomal subunit at 3.3 angstroms resolution.* Cell, 2000. **102**(5): p. 615-23.
7. Fischer, N., et al., *Structure of the E. coli ribosome-EF-Tu complex at <3 A resolution by Cs-corrected cryo-EM.* Nature, 2015. **520**(7548): p. 567-70.
8. Forchhammer, J. and L. Lindahl, *Growth rate of polypeptide chains as a function of the cell growth rate in a mutant of Escherichia coli 15.* J Mol Biol, 1971. **55**(3): p. 563-8.
9. Antoun, A., et al., *How initiation factors tune the rate of initiation of protein synthesis in bacteria.* EMBO J, 2006. **25**(11): p. 2539-50.
10. Antoun, A., et al., *How initiation factors maximize the accuracy of tRNA selection in initiation of bacterial protein synthesis.* Mol Cell, 2006. **23**(2): p. 183-93.
11. Pavlov, M.Y., et al., *Activation of initiation factor 2 by ligands and mutations for rapid docking of ribosomal subunits.* EMBO J, 2011. **30**(2): p. 289-301.
12. Goyal, A., et al., *Directional transition from initiation to elongation in bacterial translation.* Nucleic Acids Res, 2015. **43**(22): p. 10700-12.

13. Li, G.W., et al., *Quantifying absolute protein synthesis rates reveals principles underlying allocation of cellular resources.* Cell, 2014. **157**(3): p. 624-35.
14. Salis, H.M., E.A. Mirsky, and C.A. Voigt, *Automated design of synthetic ribosome binding sites to control protein expression.* Nat Biotechnol, 2009. **27**(10): p. 946-50.
15. Valle, M., et al., *Incorporation of aminoacyl-tRNA into the ribosome as seen by cryo-electron microscopy.* Nat Struct Biol, 2003. **10**(11): p. 899-906.
16. Johansson, M., M. Lovmar, and M. Ehrenberg, *Rate and accuracy of bacterial protein synthesis revisited.* Curr Opin Microbiol, 2008. **11**(2): p. 141-7.
17. Li, G.W., E. Oh, and J.S. Weissman, *The anti-Shine-Dalgarno sequence drives translational pausing and codon choice in bacteria.* Nature, 2012. **484**(7395): p. 538-41.
18. Subramaniam, A.R., B.M. Zid, and E.K. O'Shea, *An integrated approach reveals regulatory controls on bacterial translation elongation.* Cell, 2014. **159**(5): p. 1200-11.
19. Valle, M., et al., *Locking and unlocking of ribosomal motions.* Cell, 2003. **114**(1): p. 123-34.
20. Moazed, D. and H.F. Noller, *Intermediate states in the movement of transfer RNA in the ribosome.* Nature, 1989. **342**(6246): p. 142-8.
21. Frank, J. and R.K. Agrawal, *A ratchet-like inter-subunit reorganization of the ribosome during translocation.* Nature, 2000. **406**(6793): p. 318-22.
22. Agirrezabala, X., et al., *Structural characterization of mRNA-tRNA translocation intermediates.* Proc Natl Acad Sci U S A, 2012. **109**(16): p. 6094-9.
23. Spiegel, P.C., D.N. Ermolenko, and H.F. Noller, *Elongation factor G stabilizes the hybrid-state conformation of the 70S ribosome.* RNA, 2007. **13**(9): p. 1473-82.
24. Ermolenko, D.N., et al., *Observation of intersubunit movement of the ribosome in solution using FRET.* J Mol Biol, 2007. **370**(3): p. 530-40.
25. Munro, J.B., et al., *A fast dynamic mode of the EF-G-bound ribosome.* EMBO J, 2010. **29**(4): p. 770-81.
26. Pestka, S., *Studies on the formation of trensfer ribonucleic acid-ribosome complexes. V. On the function of a soluble transfer factor in protein synthesis.* Proc Natl Acad Sci U S A, 1968. **61**(2): p. 726-33.
27. Gavrilova, L.P. and A.S. Spirin, *Stimulation of "non-enzymic" translocation in ribosomes by p-chloromercuribenzoate.* FEBS Lett, 1971. **17**(2): p. 324-326.

28. Rodnina, M.V., et al., *Hydrolysis of GTP by elongation factor G drives tRNA movement on the ribosome.* Nature, 1997. **385**(6611): p. 37-41.
29. Modolell, J., Vazquez, D., in *MTP International Review of Science, Biochemistry: Synthesis of Amino Acids and Proteins*, H.L. Kornberg, Phillips, D.C., Arnstein, H.R.V., Editor. 1975, Butterworth: London. p. 137-178.
30. Nishizuka, Y. and F. Lipmann, *The interrelationship between guanosine triphosphatase and amino acid polymerization.* Arch Biochem Biophys, 1966. **116**(1): p. 344-51.
31. Spirin, A.S., *The ribosome as an RNA-based molecular machine.* RNA Biol, 2004. **1**(1): p. 3-9.
32. Ermolenko, D.N. and H.F. Noller, *mRNA translocation occurs during the second step of ribosomal intersubunit rotation.* Nat Struct Mol Biol, 2011. **18**(4): p. 457-62.
33. Modolell, J., T. Girbes, and D. Vazquez, *Ribosomal translocation promoted by guanylylimido diphosphate and guanylyl-methylene diphosphonate.* FEBS Lett, 1975. **60**(1): p. 109-13.
34. Salsi, E., E. Farah, and D.N. Ermolenko, *EF-G Activation by Phosphate Analogs.* J Mol Biol, 2016. **428**(10 Pt B): p. 2248-58.
35. Holtkamp, W., et al., *GTP hydrolysis by EF-G synchronizes tRNA movement on small and large ribosomal subunits.* EMBO J, 2014. **33**(9): p. 1073-85.
36. Chen, C., et al., *Elongation factor G initiates translocation through a power stroke.* Proc Natl Acad Sci U S A, 2016. **113**(27): p. 7515-20.
37. Belardinelli, R., et al., *Choreography of molecular movements during ribosome progression along mRNA.* Nat Struct Mol Biol, 2016. **23**(4): p. 342-8.
38. Wasserman, M.R., et al., *Multiperspective smFRET reveals rate-determining late intermediates of ribosomal translocation.* Nat Struct Mol Biol, 2016. **23**(4): p. 333-41.
39. Ratje, A.H., et al., *Head swivel on the ribosome facilitates translocation by means of intra-subunit tRNA hybrid sites.* Nature, 2010. **468**(7324): p. 713-6.
40. Guo, Z. and H.F. Noller, *Rotation of the head of the 30S ribosomal subunit during mRNA translocation.* Proc Natl Acad Sci U S A, 2012. **109**(50): p. 20391-4.
41. Fei, J., et al., *Coupling of ribosomal L1 stalk and tRNA dynamics during translation elongation.* Mol Cell, 2008. **30**(3): p. 348-59.
42. Horan, L.H. and H.F. Noller, *Intersubunit movement is required for ribosomal translocation.* Proc Natl Acad Sci U S A, 2007. **104**(12): p. 4881-5.

43. Subramanian, A.R. and E.R. Dabbs, *Functional studies on ribosomes lacking protein L1 from mutant Escherichia coli.* Eur J Biochem, 1980. **112**(2): p. 425-30.
44. Borg, A. and M. Ehrenberg, *Determinants of the rate of mRNA translocation in bacterial protein synthesis.* J Mol Biol, 2015. **427**(9): p. 1835-47.
45. Scolnick, E., et al., *Release factors differing in specificity for terminator codons.* Proc Natl Acad Sci U S A, 1968. **61**(2): p. 768-74.
46. Povolotskaya, I.S., et al., *Stop codons in bacteria are not selectively equivalent.* Biol Direct, 2012. **7**: p. 30.
47. Korkmaz, G., et al., *Comprehensive analysis of stop codon usage in bacteria and its correlation with release factor abundance.* J Biol Chem, 2014. **289**(44): p. 30334-42.
48. Freistroffer, D.V., et al., *Release factor RF3 in E.coli accelerates the dissociation of release factors RF1 and RF2 from the ribosome in a GTP-dependent manner.* EMBO J, 1997. **16**(13): p. 4126-33.
49. Zavialov, A.V., R.H. Buckingham, and M. Ehrenberg, *A posttermination ribosomal complex is the guanine nucleotide exchange factor for peptide release factor RF3.* Cell, 2001. **107**(1): p. 115-24.
50. Hirashima, A. and A. Kaji, *Role of elongation factor G and a protein factor on the release of ribosomes from messenger ribonucleic acid.* J Biol Chem, 1973. **248**(21): p. 7580-7.
51. Borg, A., M. Pavlov, and M. Ehrenberg, *Complete kinetic mechanism for recycling of the bacterial ribosome.* RNA, 2016. **22**(1): p. 10-21.
52. Janosi, L., et al., *Evidence for in vivo ribosome recycling, the fourth step in protein biosynthesis.* EMBO J, 1998. **17**(4): p. 1141-51.
53. Orelle, C., et al., *Protein synthesis by ribosomes with tethered subunits.* Nature, 2015. **524**(7563): p. 119-24.
54. Fried, S.D., et al., *Ribosome Subunit Stapling for Orthogonal Translation in E. coli.* Angew Chem Int Ed Engl, 2015. **54**(43): p. 12791-4.
55. Yamamoto, H., et al., *70S-scanning initiation is a novel and frequent initiation mode of ribosomal translation in bacteria.* Proc Natl Acad Sci U S A, 2016. **113**(9): p. E1180-9.
56. Das, B., S. Chattopadhyay, and C. Das Gupta, *Reactivation of denatured fungal glucose 6-phosphate dehydrogenase and E. coli alkaline phosphatase with E. coli ribosome.* Biochem Biophys Res Commun, 1992. **183**(2): p. 774-80.
57. Chattopadhyay, S., B. Das, and C. Dasgupta, *Reactivation of denatured proteins by 23S ribosomal RNA: role of domain V.* Proc Natl Acad Sci U S A, 1996. **93**(16): p. 8284-7.

58. Pang, Y., et al., *The antiprion compound 6-aminophenanthridine inhibits the protein folding activity of the ribosome by direct competition.* J Biol Chem, 2013. **288**(26): p. 19081-9.
59. Zhang, G., M. Hubalewska, and Z. Ignatova, *Transient ribosomal attenuation coordinates protein synthesis and co-translational folding.* Nat Struct Mol Biol, 2009. **16**(3): p. 274-80.
60. O'Brien, E.P., M. Vendruscolo, and C.M. Dobson, *Kinetic modelling indicates that fast-translating codons can coordinate cotranslational protein folding by avoiding misfolded intermediates.* Nat Commun, 2014. **5**: p. 2988.
61. Nissley, D.A., et al., *Accurate prediction of cellular co-translational folding indicates proteins can switch from post- to co-translational folding.* Nat Commun, 2016. **7**: p. 10341.
62. Sander, I.M., J.L. Chaney, and P.L. Clark, *Expanding Anfinsen's principle: contributions of synonymous codon selection to rational protein design.* J Am Chem Soc, 2014. **136**(3): p. 858-61.
63. Poehlsgaard, J. and S. Douthwaite, *The bacterial ribosome as a target for antibiotics.* Nat Rev Microbiol, 2005. **3**(11): p. 870-81.
64. Wilson, D.N., *Ribosome-targeting antibiotics and mechanisms of bacterial resistance.* Nat Rev Microbiol, 2014. **12**(1): p. 35-48.
65. Wilson, D.N., *The A-Z of bacterial translation inhibitors.* Crit Rev Biochem Mol Biol, 2009. **44**(6): p. 393-433.
66. Finlay, A.C., et al., *Viomycin a new antibiotic active against Mycobacteria.* Am Rev Tuberc, 1951. **63**(1): p. 1-3.
67. Bartz, Q.R., et al., *Viomycin, a new tuberculostatic antibiotic.* Am Rev Tuberc, 1951. **63**(1): p. 4-6.
68. Thomas, M.G., Y.A. Chan, and S.G. Ozanick, *Deciphering tuberactinomycin biosynthesis: isolation, sequencing, and annotation of the viomycin biosynthetic gene cluster.* Antimicrob Agents Chemother, 2003. **47**(9): p. 2823-30.
69. Marrero, P., M.J. Cabanas, and J. Modolell, *Induction of translational errors (misreading) by tuberactinomycins and capreomycins.* Biochem Biophys Res Commun, 1980. **97**(3): p. 1047-42.
70. Modolell, J. and Vazquez, *The inhibition of ribosomal translocation by viomycin.* Eur J Biochem, 1977. **81**(3): p. 491-7.
71. Stanley, R.E., et al., *The structures of the anti-tuberculosis antibiotics viomycin and capreomycin bound to the 70S ribosome.* Nat Struct Mol Biol, 2010. **17**(3): p. 289-93.
72. Ermolenko, D.N., et al., *The antibiotic viomycin traps the ribosome in an intermediate state of translocation.* Nat Struct Mol Biol, 2007. **14**(6): p. 493-7.
73. Pulk, A. and J.H. Cate, *Control of ribosomal subunit rotation by elongation factor G.* Science, 2013. **340**(6140): p. 1235970.

74. Brilot, A.F., et al., *Structure of the ribosome with elongation factor G trapped in the pretranslocation state.* Proc Natl Acad Sci U S A, 2013. **110**(52): p. 20994-9.
75. Godtfredsen, W.O., et al., *Fusidic acid: a new antibiotic.* Nature, 1962. **193**: p. 987.
76. Cundliffe, E., *The mode of action of fusidic acid.* Biochem Biophys Res Commun, 1972. **46**(5): p. 1794-801.
77. Gao, Y.G., et al., *The structure of the ribosome with elongation factor G trapped in the posttranslocational state.* Science, 2009. **326**(5953): p. 694-9.
78. Ramrath, D.J., et al., *Visualization of two transfer RNAs trapped in transit during elongation factor G-mediated translocation.* Proc Natl Acad Sci U S A, 2013. **110**(52): p. 20964-9.
79. Parker, J., *Errors and alternatives in reading the universal genetic code.* Microbiol Rev, 1989. **53**(3): p. 273-98.
80. Kramer, E.B. and P.J. Farabaugh, *The frequency of translational misreading errors in E. coli is largely determined by tRNA competition.* RNA, 2007. **13**(1): p. 87-96.
81. Manickam, N., et al., *Studies of translational misreading in vivo show that the ribosome very efficiently discriminates against most potential errors.* RNA, 2014. **20**(1): p. 9-15.
82. Fersht, A., *Structure and Mechanism in Protein Science*. 1998, New York: W. H. Freeman and Company.
83. Dong, H., L. Nilsson, and C.G. Kurland, *Co-variation of tRNA abundance and codon usage in Escherichia coli at different growth rates.* J Mol Biol, 1996. **260**(5): p. 649-63.
84. Pauling, L., *The Probability of Errors in the Process of Synthesis of Protein Molecules*, in *Festschrift Arthur Stoll*. 1957, Birkhäuse Verlag: Basel. p. 597-602.
85. Ninio, J., *A semi-quantitative treatment of missense and nonsense suppression in the strA and ram ribosomal mutants of Escherichia coli. Evaluation of some molecular parameters of translation in vivo.* J Mol Biol, 1974. **84**(2): p. 297-313.
86. Johansson, M., J. Zhang, and M. Ehrenberg, *Genetic code translation displays a linear trade-off between efficiency and accuracy of tRNA selection.* Proc Natl Acad Sci U S A, 2012. **109**(1): p. 131-6.
87. Hopfield, J.J., *Kinetic proofreading: a new mechanism for reducing errors in biosynthetic processes requiring high specificity.* Proc Natl Acad Sci U S A, 1974. **71**(10): p. 4135-9.
88. Ninio, J., *Kinetic amplification of enzyme discrimination.* Biochimie, 1975. **57**(5): p. 587-95.
89. Ehrenberg, M. and C. Blomberg, *Thermodynamic constraints on kinetic proofreading in biosynthetic pathways.* Biophys J, 1980. **31**(3): p. 333-58.

90. Thompson, R.C. and P.J. Stone, *Proofreading of the codon-anticodon interaction on ribosomes.* Proc Natl Acad Sci U S A, 1977. **74**(1): p. 198-202.
91. Ruusala, T., M. Ehrenberg, and C.G. Kurland, *Is there proofreading during polypeptide synthesis?* EMBO J, 1982. **1**(6): p. 741-5.
92. Johansson, M., et al., *The kinetics of ribosomal peptidyl transfer revisited.* Mol Cell, 2008. **30**(5): p. 589-98.
93. Zhang, J., et al., *Accuracy of initial codon selection by aminoacyl-tRNAs on the mRNA-programmed bacterial ribosome.* Proc Natl Acad Sci U S A, 2015. **112**(31): p. 9602-7.
94. Zhang, J., et al., *Proofreading neutralizes potential error hotspots in genetic code translation by transfer RNAs.* RNA, 2016. **22**(6): p. 896-904.
95. Rodnina, M.V., et al., *Initial binding of the elongation factor Tu.GTP.aminoacyl-tRNA complex preceding codon recognition on the ribosome.* J Biol Chem, 1996. **271**(2): p. 646-52.
96. Pape, T., W. Wintermeyer, and M. Rodnina, *Induced fit in initial selection and proofreading of aminoacyl-tRNA on the ribosome.* EMBO J, 1999. **18**(13): p. 3800-7.
97. Gromadski, K.B. and M.V. Rodnina, *Kinetic determinants of high-fidelity tRNA discrimination on the ribosome.* Mol Cell, 2004. **13**(2): p. 191-200.
98. Gromadski, K.B., T. Daviter, and M.V. Rodnina, *A uniform response to mismatches in codon-anticodon complexes ensures ribosomal fidelity.* Mol Cell, 2006. **21**(3): p. 369-77.
99. Geggier, P., et al., *Conformational sampling of aminoacyl-tRNA during selection on the bacterial ribosome.* J Mol Biol, 2010. **399**(4): p. 576-95.
100. Ogle, J.M., et al., *Recognition of cognate transfer RNA by the 30S ribosomal subunit.* Science, 2001. **292**(5518): p. 897-902.
101. Carter, A.P., et al., *Functional insights from the structure of the 30S ribosomal subunit and its interactions with antibiotics.* Nature, 2000. **407**(6802): p. 340-8.
102. Ogle, J.M., et al., *Selection of tRNA by the ribosome requires a transition from an open to a closed form.* Cell, 2002. **111**(5): p. 721-32.
103. Ogle, J.M., A.P. Carter, and V. Ramakrishnan, *Insights into the decoding mechanism from recent ribosome structures.* Trends Biochem Sci, 2003. **28**(5): p. 259-66.
104. Demeshkina, N., et al., *A new understanding of the decoding principle on the ribosome.* Nature, 2012. **484**(7393): p. 256-9.
105. Rozov, A., et al., *Structural insights into the translational infidelity mechanism.* Nat Commun, 2015. **6**: p. 7251.

106. Satpati, P., J. Sund, and J. Aqvist, *Structure-based energetics of mRNA decoding on the ribosome.* Biochemistry, 2014. **53**(10): p. 1714-22.
107. Zeng, X., et al., *Flipping of the ribosomal A-site adenines provides a basis for tRNA selection.* J Mol Biol, 2014. **426**(19): p. 3201-13.
108. Koshland, D.E., *Application of a Theory of Enzyme Specificity to Protein Synthesis.* Proc Natl Acad Sci U S A, 1958. **44**(2): p. 98-104.
109. Pavlov, M.Y. and M. Ehrenberg, *Rate of translation of natural mRNAs in an optimized in vitro system.* Arch Biochem Biophys, 1996. **328**(1): p. 9-16.
110. Jelenc, P.C. and C.G. Kurland, *Nucleoside triphosphate regeneration decreases the frequency of translation errors.* Proc Natl Acad Sci U S A, 1979. **76**(7): p. 3174-8.
111. Alatossava, T., et al., *Manipulation of intracellular magnesium content in polymyxin B nonapeptide-sensitized Escherichia coli by ionophore A23187.* J Bacteriol, 1985. **162**(1): p. 413-9.
112. Mandava, C.S., et al., *Bacterial ribosome requires multiple L12 dimers for efficient initiation and elongation of protein synthesis involving IF2 and EF-G.* Nucleic Acids Res, 2012. **40**(5): p. 2054-64.
113. Indrisiunaite, G., et al., *On the pH dependence of class-1 RF-dependent termination of mRNA translation.* J Mol Biol, 2015. **427**(9): p. 1848-60.
114. Studer, S.M., J.S. Feinberg, and S. Joseph, *Rapid kinetic analysis of EF-G-dependent mRNA translocation in the ribosome.* J Mol Biol, 2003. **327**(2): p. 369-81.
115. Tanaka, N., T. Kinoshita, and H. Masukawa, *Mechanism of protein synthesis inhibition by fusidic acid and related antibiotics.* Biochem Biophys Res Commun, 1968. **30**(3): p. 278-83.
116. Burns, K., M. Cannon, and E. Cundliffe, *A resolution of conflicting reports concerning the mode of action of fusidic acid.* FEBS Lett, 1974. **40**(1): p. 219-23.
117. Bodley, J.W., F.J. Zieve, and L. Lin, *Studies on translocation. IV. The hydrolysis of a single round of guanosine triphosphate in the presence of fusidic acid.* J Biol Chem, 1970. **245**(21): p. 5662-7.
118. Willie, G.R., et al., *Some characteristics of and structural requirements for the interaction of 24,25-dihydrofusidic acid with ribosome - elongation factor g Complexes.* Biochemistry, 1975. **14**(8): p. 1713-8.
119. Chen, J., et al., *Coordinated conformational and compositional dynamics drive ribosome translocation.* Nat Struct Mol Biol, 2013. **20**(6): p. 718-27.

120. Zhou, J., et al., *Crystal structures of EF-G-ribosome complexes trapped in intermediate states of translocation.* Science, 2013. **340**(6140): p. 1236086.
121. Connell, S.R., et al., *Structural basis for interaction of the ribosome with the switch regions of GTP-bound elongation factors.* Mol Cell, 2007. **25**(5): p. 751-64.
122. Lin, J., et al., *Conformational changes of elongation factor G on the ribosome during tRNA translocation.* Cell, 2015. **160**(1-2): p. 219-27.
123. Savelsbergh, A., M.V. Rodnina, and W. Wintermeyer, *Distinct functions of elongation factor G in ribosome recycling and translocation.* RNA, 2009. **15**(5): p. 772-80.
124. Borg, A., M. Pavlov, and M. Ehrenberg, *Mechanism of fusidic acid inhibition of RRF- and EF-G-dependent splitting of the bacterial post-termination ribosome.* Nucleic Acids Res, 2016. **44**(7): p. 3264-75.
125. Sala, F. and O. Ciferri, *Inhibition of peptide chain initiation in Escherichia coli by fusidic acid.* Biochim Biophys Acta, 1970. **224**(1): p. 199-205.
126. Liou, Y.F. and N. Tanaka, *Dual actions of viomycin on the ribosomal functions.* Biochem Biophys Res Commun, 1976. **71**(2): p. 477-83.
127. Feldman, M.B., et al., *Aminoglycoside activity observed on single pre-translocation ribosome complexes.* Nat Chem Biol, 2010. **6**(1): p. 54-62.
128. Martinez, O., D. Vazquez, and J. Modolell, *Streptomycin- and viomycin-induced conformational changes of ribosomes detected by iodination.* FEBS Lett, 1978. **87**(1): p. 21-5.
129. Cornish, P.V., et al., *Spontaneous intersubunit rotation in single ribosomes.* Mol Cell, 2008. **30**(5): p. 578-88.
130. Zhou, J., et al., *Crystal structure of release factor RF3 trapped in the GTP state on a rotated conformation of the ribosome.* RNA, 2012. **18**(2): p. 230-40.
131. Kim, H.D., J.D. Puglisi, and S. Chu, *Fluctuations of transfer RNAs between classical and hybrid states.* Biophys J, 2007. **93**(10): p. 3575-82.
132. Lambert, J.M., et al., *Levels of ribosomal protein S1 and elongation factor G in the growth cycle of Escherichia coli.* J Bacteriol, 1983. **154**(3): p. 1323-8.
133. Ning, W., J. Fei, and R.L. Gonzalez, Jr., *The ribosome uses cooperative conformational changes to maximize and regulate the efficiency of translation.* Proc Natl Acad Sci U S A, 2014. **111**(33): p. 12073-8.

134. Davies, J., L. Gorini, and B.D. Davis, *Misreading of RNA codewords induced by aminoglycoside antibiotics.* Mol Pharmacol, 1965. **1**(1): p. 93-106.
135. Akbergenov, R., et al., *Molecular basis for the selectivity of antituberculosis compounds capreomycin and viomycin.* Antimicrob Agents Chemother, 2011. **55**(10): p. 4712-7.
136. Matt, T., et al., *Dissociation of antibacterial activity and aminoglycoside ototoxicity in the 4-monosubstituted 2-deoxystreptamine apramycin.* Proc Natl Acad Sci U S A, 2012. **109**(27): p. 10984-9.
137. Korostelev, A., et al., *Crystal structure of a 70S ribosome-tRNA complex reveals functional interactions and rearrangements.* Cell, 2006. **126**(6): p. 1065-77.
138. Schuwirth, B.S., et al., *Structures of the bacterial ribosome at 3.5 A resolution.* Science, 2005. **310**(5749): p. 827-34.
139. Fourmy, D., et al., *Structure of the A site of Escherichia coli 16S ribosomal RNA complexed with an aminoglycoside antibiotic.* Science, 1996. **274**(5291): p. 1367-71.
140. Fourmy, D., S. Yoshizawa, and J.D. Puglisi, *Paromomycin binding induces a local conformational change in the A-site of 16 S rRNA.* J Mol Biol, 1998. **277**(2): p. 333-45.
141. Sanbonmatsu, K.Y., *Energy landscape of the ribosomal decoding center.* Biochimie, 2006. **88**(8): p. 1053-9.
142. Vaiana, A.C. and K.Y. Sanbonmatsu, *Stochastic gating and drug-ribosome interactions.* J Mol Biol, 2009. **386**(3): p. 648-61.
143. Schmeing, T.M., et al., *How mutations in tRNA distant from the anticodon affect the fidelity of decoding.* Nat Struct Mol Biol, 2011. **18**(4): p. 432-6.
144. Sanbonmatsu, K.Y. and S. Joseph, *Understanding discrimination by the ribosome: stability testing and groove measurement of codon-anticodon pairs.* J Mol Biol, 2003. **328**(1): p. 33-47.
145. Maus, C.E., B.B. Plikaytis, and T.M. Shinnick, *Mutation of tlyA confers capreomycin resistance in Mycobacterium tuberculosis.* Antimicrob Agents Chemother, 2005. **49**(2): p. 571-7.
146. Johansen, S.K., et al., *Capreomycin binds across the ribosomal subunit interface using tlyA-encoded 2'-O-methylations in 16S and 23S rRNAs.* Mol Cell, 2006. **23**(2): p. 173-82.
147. Monshupanee, T., et al., *Capreomycin susceptibility is increased by TlyA-directed 2'-O-methylation on both ribosomal subunits.* Mol Microbiol, 2012. **85**(6): p. 1194-203.
148. Fange, D., et al., *Drug efflux pump deficiency and drug target resistance masking in growing bacteria.* Proc Natl Acad Sci U S A, 2009. **106**(20): p. 8215-20.

149. Deris, J.B., et al., *The innate growth bistability and fitness landscapes of antibiotic-resistant bacteria.* Science, 2013. **342**(6162): p. 1237435.
150. Eyal, Z., et al., *Structural insights into species-specific features of the ribosome from the pathogen Staphylococcus aureus.* Proc Natl Acad Sci U S A, 2015. **112**(43): p. E5805-14.
151. Ehrenberg, M., H. Bremer, and P.P. Dennis, *Medium-dependent control of the bacterial growth rate.* Biochimie, 2013. **95**(4): p. 643-58.
152. Maitra, A. and K.A. Dill, *Modeling the Overproduction of Ribosomes when Antibacterial Drugs Act on Cells.* Biophys J, 2016. **110**(3): p. 743-8.
153. Kannan, K., et al., *The general mode of translation inhibition by macrolide antibiotics.* Proc Natl Acad Sci U S A, 2014. **111**(45): p. 15958-63.
154. Sothiselvam, S., et al., *Macrolide antibiotics allosterically predispose the ribosome for translation arrest.* Proc Natl Acad Sci U S A, 2014. **111**(27): p. 9804-9.

Acta Universitatis Upsaliensis

Digital Comprehensive Summaries of Uppsala Dissertations from the Faculty of Science and Technology 1399

Editor: The Dean of the Faculty of Science and Technology

A doctoral dissertation from the Faculty of Science and Technology, Uppsala University, is usually a summary of a number of papers. A few copies of the complete dissertation are kept at major Swedish research libraries, while the summary alone is distributed internationally through the series Digital Comprehensive Summaries of Uppsala Dissertations from the Faculty of Science and Technology. (Prior to January, 2005, the series was published under the title "Comprehensive Summaries of Uppsala Dissertations from the Faculty of Science and Technology".)

Distribution: publications.uu.se
urn:nbn:se:uu:diva-300479

ACTA
UNIVERSITATIS
UPSALIENSIS
UPPSALA
2016